Dip moveout of converted waves and parameter estimation in transversely isotropic media

Ilya Tsvankin* **and Vladimir Grechka***

*Center for Wave Phenomena, Department of Geophysics, Colorado School of Mines, Golden, CO 80401-1887, USA

ABSTRACT

For transverse isotropy with a vertical symmetry axis (VTI media), P-wave reflection data alone are insufficient for building velocity models in *depth*. Here, we show that all parameters of VTI media responsible for propagation of P- and SV-waves (the P-wave and S-wave vertical velocities V_{P0} and V_{S0} and the anisotropic parameters ϵ and δ) can be obtained by combining P-wave traveltimes with the moveout of PS-waves converted at a horizontal and dipping interface. Using converted modes, rather than pure S-waves, avoids the need for expensive shear-wave excitation on land and makes the method suitable for offshore exploration.

The inversion algorithm is based on a new analytic description of the dip moveout of PS-waves developed for symmetry planes of anisotropic media (and for any vertical plane in models with *weak* azimuthal anisotropy). The common-midpoint (CMP) traveltime-offset relationship, derived in a parametric form and represented through the components of the slowness vector of the P and S-waves, makes it possible to compute the moveout curve of the PS-wave without two-point ray tracing. This formalism also leads to closed-form solutions for moveout attributes, such as the coordinates ($x_{\min}$, $t_{\min}$) of the traveltime minimum, the normal-moveout (NMO) velocity defined at $x = x_{\min}$ and the slope of the moveout curve (apparent slowness) at zero offset.

The parameter-estimation algorithm operates with reflection moveout of P- and PS-waves from a horizontal and dipping reflector. The NMO velocities of P and PS-waves from horizontal events and the ratio of the corresponding zero-offset traveltimes yield three equations for the four unknown medium parameters. The remaining parameter is found from an overdetermined system of equations that includes the P-wave NMO velocity and moveout attributes of the PS-wave for a dipping event. Numerical analysis shows that the PS-wave dip-moveout signature plays a crucial role in obtaining accurate estimates of the anisotropic parameters. The joint inver-

sion of P and PS data provides the necessary information not only for P-wave depth imaging in VTI media, but also for the processing of PS-waves, including re-sorting of PS traces into common-reflection-point gathers and transformation to zero offset (TZO).

Keywords.—converted wave, seismic anisotropy, seismic inversion, reflection moveout.

INTRODUCTION

Recent advances in the development and application of anisotropic processing algorithms (e.g., Alkhalifah et al. 1996) were made possible by new approaches to the inversion of surface seismic data for the anisotropic parameters. Alkhalifah and Tsvankin (1995) showed that P-wave[1] reflection moveout and all time-processing steps [NMO and dip-moveout (DMO) corrections, prestack and poststack time migration] in horizontally layered VTI media above a dipping reflector depend on just two parameters – the normal-moveout velocity from a horizontal reflector $V_{\mathrm{nmo},P}(0)$ and the "anellipticity" coefficient η. In terms of Thomsen's (1986) parameters, $V_{\mathrm{nmo},P}(0)$ and η are given by

$$V_{\mathrm{nmo},P}(0) = V_{P0}\sqrt{1+2\delta}\,, \tag{1}$$

$$\eta = \frac{\epsilon-\delta}{1+2\delta}\,, \tag{2}$$

where V_{P0} is the P-wave vertical velocity, and ϵ and δ are the anisotropic parameters responsible for the velocities of P- and SV-waves. [V_{P0}, ϵ and δ are sufficient to determine all kinematic signatures of P-waves, while SV-wave kinematics also depends on the shear-wave vertical velocity V_{S0} (Tsvankin 1996).] Both $V_{\mathrm{nmo},P}(0)$ and η can be found from surface P-wave data using either the dip dependence of NMO velocity or nonhyperbolic (long-spread) moveout of horizontal events (Alkhalifah and Tsvankin 1995; Grechka and Tsvankin 1998).

P-wave depth processing (such as prestack depth migration), however, requires knowledge of the vertical velocity V_{P0}. Only if the symmetry axis of TI media is tilted by at least 30-40° from vertical, can azimuthally dependent P-wave NMO velocity from two or more reflectors with different dips and/or azimuths be inverted for all

[1]For brevity, the qualifiers in "quasi-P-wave" and "quasi-S-wave" will be omitted.

parameters which control P-wave kinematics (Grechka and Tsvankin 1999). Thus, to resolve the vertical velocity and the anisotropic parameters of VTI media, it is necessary to supplement P-wave traveltimes with additional data. Since the SV-wave velocity also depends on the anisotropic parameters ϵ and δ, a natural option is to include reflection moveout of SV-waves into the inversion procedure. Tsvankin and Thomsen (1995) suggested combining long-spread (nonhyperbolic) moveout of P- and SV-waves from horizontal reflectors to obtain all four parameters, but their approach encounters practical problems stemming from difficulties in acquiring and processing of long-spread shear data.

Alternatively, input data may include dip-dependent P-wave moveout (e.g., NMO velocities for two different dips), yielding the parameters $V_{\mathrm{nmo},P}(0)$ and η, and the NMO velocity of the SV-wave from a horizontal reflector:

$$V_{\mathrm{nmo},SV} = V_{S0}\,\sqrt{1+2\sigma}\,, \tag{3}$$

$$\sigma \equiv \left(\frac{V_{P0}}{V_{S0}}\right)^2 (\epsilon - \delta)\,. \tag{4}$$

If pure shear waves are not excited, the SV-wave NMO velocity can be determined from the NMO velocities of the P- and converted PSV-waves (here denoted simply as PS) in the following way (Seriff and Sriram 1991):

$$t_{PS0}\,V^2_{\mathrm{nmo},PS} = t_{P0}\,V^2_{\mathrm{nmo},P} + t_{S0}\,V^2_{\mathrm{nmo},SV}\,, \tag{5}$$

where t_{P0} and t_{S0} are the vertical traveltimes of the P and S-waves, and $t_{PS0} = t_{P0} + t_{S0}$. Also, if either S- or PS-waves are available, the ratio of the vertical velocities can be found from the vertical traveltimes:

$$\frac{V_{P0}}{V_{S0}} = \frac{t_{S0}}{t_{P0}}\,. \tag{6}$$

In principle, equations (1), (2), (3), and (6) are sufficient to recover all four unknown parameters (V_{P0}, V_{S0}, ϵ and δ). In vertically inhomogeneous media, the interval NMO

velocities [equations (1) and (3)] can be found from the conventional Dix equation and combined with the interval η [equation (2)] to perform parameter estimation.

Unfortunately, this inversion procedure turns out to be unstable, with realistic small errors in the input data propagating with considerable amplification into the inverted vertical velocities, ϵ, and δ (Grechka and Tsvankin 1999). This instability is caused by the form of the dependence of SV-wave NMO velocity on the anisotropic parameters [equations (3) and (4)]. After obtaining $\eta \approx \epsilon - \delta$ from P-wave data and V_{P0}/V_{S0} from the vertical traveltimes, equation (3) can be used to find the S-wave vertical velocity. However, the multiplier $(V_{P0}/V_{S0})^2$ translates small errors in $\epsilon - \delta$ into substantially larger errors in σ and V_{S0}. For a typical $V_{P0}/V_{S0} = 2$, a relatively insignificant error of 0.03 in $\epsilon - \delta$ will cause a distortion of 0.12 in σ and an error of up to 12% in V_{S0} and, consequently, in V_{P0}.

Here, we suggest a more stable parameter-estimation algorithm based on including dip-dependent reflection traveltimes of mode-converted PS-waves in the inversion procedure. Previous work on reflection moveout of converted waves was mostly restricted to isotropic media (e.g., Tessmer and Behle 1988; Alfaraj 1993). Equation (5) for NMO velocity of PS-waves in horizontally layered VTI media was first given by Seriff and Sriram (1991). Tsvankin and Thomsen (1994) presented an analytic expression for the quartic moveout term of PS conversions for vertical transverse isotropy and used it to describe nonhyperbolic (long-spread) reflection moveout. Anderson (1996) developed a TZO (transformation to zero offset) algorithm for vertical transverse isotropy that produces a zero-offset P-wave section from PS data. Grechka, Theophanis and Tsvankin (1999) showed that the azimuthal variation of NMO velocity of converted waves in horizontally layered anisotropic media with a horizontal symmetry plane always has an elliptical form [the result previously proved by Grechka and Tsvankin (1998) for pure modes]. They also generalized relationship (5) between the NMO velocities of pure and converted waves to azimuthally anisotropic media and combined NMO and vertical velocities of P and PS-waves to obtain the parameters

of a horizontal orthorhombic layer.

We begin by giving a general analytic description of dip-dependent reflection moveout for converted waves in a symmetry plane of a homogeneous anisotropic layer. This formalism leads to closed-form expressions for the moveout curve and its attributes (such as NMO velocity near the traveltime minimum and the shift of the traveltime minimum from zero offset) in terms of the horizontal and vertical slowness components of the P and S-waves. For vertical transverse isotropy, we employ the weak-anisotropy approximation to simplify the exact equations and explain the relationship between the moveout attributes and medium parameters. Then we use the exact equations (for arbitrary strength of the anisotropy) to perform joint inversion of the P- and PS-wave moveout from a horizontal and dipping reflector and show that the new method yields stable estimates of the vertical velocities and anisotropic parameters of VTI media. Although the inversion algorithm is developed for vertical transverse isotropy, it remains fully valid in the vertical symmetry planes of orthorhombic media.

DIP MOVEOUT OF CONVERTED WAVES IN SYMMETRY PLANES OF ANISOTROPIC MEDIA

A key difference between reflection moveout of converted and pure modes in CMP geometry is that mode conversion makes the moveout curve asymmetric with respect to zero offset (i.e., traveltime is not an even function of offset). Only in the special case of horizontal reflectors and a medium with a horizontal symmetry plane, converted-wave (e.g., PS-wave) reflection traveltime remains the same if we interchange the source and receiver (Grechka, Theophanis and Tsvankin 1997). The asymmetry of the converted-wave moveout can be further enhanced by angular velocity variations in anisotropic media. Hence, in general the moveout of PS-waves cannot be described by the conventional traveltime series $t^2(x^2)$ that contains only even powers of the offset x.

It is convenient to distinguish between the two branches of the CMP moveout curve by introducing the notion of "positive" and "negative" offsets. Assuming that the source excites P-waves which get converted into $S(SV)$-waves at the reflector, we will call an offset positive if the source is located *downdip* with respect to the common midpoint and the receiver. Correspondingly, at negative offsets the P-wave source is moved updip with respect to the CMP.

Fig. 1 shows typical traveltime curves of the PS-wave computed for a common-midpoint (CMP) gather in the dip plane of a reflector beneath a VTI layer. The moveout becomes increasingly asymmetric with dip, and the traveltime minimum is recorded at positive offsets. For dips beyond 40°, the minimum moves to large offsets exceeding twice the CMP-reflector distance and then disappears altogether.

The general character of the converted-wave moveout in Fig. 1 is similar to that in isotropic media. The influence of anisotropy, however, may cause a shift of the minimum traveltime towards *negative* offsets (Fig. 2, $\phi = 10°$). For the model in Fig. 2, the traveltime for the P-wave source located updip from the common midpoint may be smaller than the zero-offset value (provided the dip is mild). This unusual phenomenon, caused by an increase in the SV-wave velocity with angle for positive values of σ, is explained in detail below [see equation (22)].

For even larger σ reaching 0.8-1 (uncommon, but feasible, values for shales), the wavefront of the SV-wave develops a cusp centered near an angle of 45° with vertical. Depending on the range of reflection angles recorded on a CMP gather, the PS-traveltime in this case may also contain a cusp and become multivalued (e.g., Tsvankin and Thomsen, 1994). Although the cusp is diagnostic of anisotropy, analysis of multivalued moveout curves requires a special treatment not discussed here.

The pronounced changes in the PS moveout curve with reflector dip suggest using different sets of moveout attributes for mild and steep dips. Below we give concise expressions for these moveout attributes and PS reflection traveltime as a whole.

Parametric representation of PS traveltime

Our goal here is to develop an analytic treatment of reflection moveout for converted waves in a homogeneous anisotropic layer above a dipping reflector. To make the problem two-dimensional, the incidence plane is assumed to coincide with both the dip plane of the reflector and a symmetry plane of the medium (Figure 3). [The same assumption was made by Tsvankin (1995) in his derivation of the 2-D NMO equation for pure modes.]

In the adopted "2-D" reflection model, the phase-velocity vectors and rays of reflected waves on the dip line do not deviate from the incidence plane. Also, the polarization vector of one of the split shear modes is perpendicular to the dip (incidence) plane, and that SH-wave is completely decoupled from the P- and SV-arrivals. Therefore, a P- or SV-wave incident upon the interface generates a single in-plane polarized converted mode (PS or SP).

As shown in Appendix A, the results of Grechka, Tsvankin and Cohen (1999) can be used to obtain the traveltime and source-receiver offset of a converted wave in a CMP gather (Fig. 3) as

$$t = z_{\rm CMP}\,\frac{q_P - p_P q'_P + q_S - p_S q'_S}{1 + \frac{1}{2}\tan\phi\,(q'_P + q'_S)} \tag{7}$$

and

$$x = z_{\rm CMP}\,\frac{q'_P - q'_S}{1 + \frac{1}{2}\tan\phi\,(q'_P + q'_S)}\,, \tag{8}$$

where $z_{\rm CMP}$ is the reflector depth beneath the common midpoint, p_P and p_S are the horizontal components of the slowness vector for the P- and S-waves (respectively), q_P and q_S are the vertical slownesses, and $q'_P \equiv dq_P/dp_P$, $q'_S \equiv dq_S/dp_S$. The slowness vectors of the P- and S-waves are related to each other by Snell's law at the reflector [see equation (9) below]. Note that the x_1-axis is directed updip, and the group-velocity vectors of both waves are assumed to point towards the surface (Fig. 3).

With these conventions, positive CMP offsets correspond to the P-wave source located *downdip* from the CMP. If the medium is isotropic, equations (7) and (8) become equivalent to expressions developed by Alfaraj (1993), and both t and x can be obtained explicitly as functions of the slowness projection $p_{\rm int}$ on the reflector (see Appendix A).

To determine the slowness vectors for a given value of projection $p_{\rm int}$, it is necessary to solve the Christoffel equation in the Cartesian coordinate system associated with the reflector. It is also possible to parameterize the traveltime curve by the horizontal slowness (ray parameter) of the P- or S-wave and find the ray parameter of the other wave from Snell's law [equation (C-5)]:

$$p_{\rm int} = -(p_P \cos\phi + q_P \sin\phi) = p_S \cos\phi + q_S \sin\phi\,. \tag{9}$$

As discussed below, in the computation of moveout attributes it is more efficient to operate directly with p_P and p_S without involving $p_{\rm int}$.

The derivative dq/dp for both waves can be found in a straightforward way by implicit differentiation of the Christoffel equation (Grechka, Tsvankin and Cohen 1999). Since the incidence plane is assumed to be a plane of symmetry, the Christoffel equation $q(p) = 0$ generally is quartic with respect to q. For models with a horizontal symmetry plane (e.g., VTI), however, the polynomial $q(p)$ becomes quadratic for q^2.

Although the generation of a CMP gather using equations (7) and (8) involves solving the Christoffel equation at least once for each reflection raypath, it does not require time-consuming two-point ray tracing. The analytic representation of dip moveout given here is used below to obtain the NMO velocity and other attributes of the moveout curve.

Attributes of the PS moveout function

The moveout attributes conventionally used in the traveltime inversion of pure-mode reflections include the normal-moveout (NMO) velocity and, sometimes, the

higher-order moveout terms responsible for nonhyperbolic moveout. Due to the asymmetric shape of the common-midpoint PS moveout curve with respect to zero offset, the attribute largely responsible for small-offset reflection traveltime is the slope of the moveout curve at $x = 0$. If reflector dip is mild and the PS moveout has a minimum at moderate offsets, suitable attributes are the minimum traveltime $t_{\min}$, the corresponding source-receiver offset $x_{\min} = x(t_{\min})$, and the normal-moveout velocity V_{nmo} responsible for traveltime near $x_{\min}$.

Slope of the moveout curve and position of the traveltime minimum.—In Appendix B, we show that the apparent slowness, or slope, of any moveout curve recorded in CMP geometry (dt/dx) is determined by the difference between the horizontal slownesses (ray parameters) of the incident and reflected ray measured at the source and receiver locations. This representation of moveout slope is valid in any inhomogeneous anisotropic medium if the rays in the CMP gather do not deviate from the incidence plane (i.e., the incidence plane is supposed to be a plane of mirror symmetry). The derivation of dt/dx in Appendix B can be easily modified to obtain the known expressions for data acquired in common-shot or common-receiver gathers. The slope of reflection moveout in a shot gather, for instance, is simply equal to the ray parameter of the reflected ray at the receiver location. The result for shot gathers (but not for CMP geometry) also follows from ray theory because for wavefronts excited by a fixed point source, the gradient of the traveltime at any point is equal to the slowness vector.

For PS-waves in CMP geometry, the slope of the $t(x)$ curve is given by (using sign conventions from Fig. 3)

$$\frac{dt}{dx} = \frac{1}{2}\left(p_S - p_P\right), \tag{10}$$

with the horizontal slownesses p_P and p_S measured at the source and receiver locations. Equation (10) not only provides a simple expression for the slope itself, it also helps to obtain concise solutions for NMO velocity and other attributes of the

moveout minimum.

If the medium above the reflector is horizontally homogeneous (as is the case with the single-layer model considered here), both p_P and p_S remain constant between the reflector and the surface. To find the moveout slope at zero offset, we determine p_P and p_S from Snell's law [equation (9)] and the condition $q'_P = q'_S$, which ensures that the group-velocity vectors of the P- and S-wave are parallel to each other [see equation (8)].

Equation (10) can also be used to find the slownesses $p_P^{\min}$ and $p_S^{\min}$ corresponding to the minimum of the moveout curve. Since the derivative dt/dx vanishes at the traveltime minimum,

$$p_P^{\min} = p_S^{\min} . \tag{11}$$

Note that in the special case of a horizontal reflector ($\phi = 0$), equation (11) is satisfied if the slowness vectors of the incident and reflected waves are vertical ($p_P = p_S = p_{\text{int}} = 0$). Therefore, the minimum of the converted-wave traveltime from a horizontal reflector always corresponds to the vertical *slowness vector*, but the incident and reflected *rays* are not necessarily vertical, unless the medium has a horizontal symmetry plane. This means that in general the traveltime minimum of the converted wave from a horizontal reflector is located at a non-zero offset $x_{\min} \neq 0$, although the slowness vectors of the corresponding P and S-waves are vertical.

Equation (11) also confirms the well-known fact that for a pure-mode reflection and arbitrary reflector dip, p_{int} of the traveltime minimum is equal to zero. Indeed, if $p_{\text{int}} = 0$, the slowness vectors of the incident and reflected waves are orthogonal to the interface (i.e, parallel to each other), so in the absence of mode conversion, $p_P = p_S$. As a result, for pure modes equation (11) is always satisfied at vanishing p_{int}, and the minimum traveltime is recorded at zero offset.

Using Snell's law [equation (9)] and equation (11), we obtain the following relationship between the slowness components corresponding to the traveltime minimum:

$$2p_P^{\min} = -(q_P + q_S)\tan\phi\,. \tag{12}$$

The vertical slownesses q_P and q_S can be found as functions of $p_P = p_S$ from the Christoffel equation. Therefore, equation (12) can be solved in a straightforward way for the horizontal slowness $p_P^{\min} = p_S^{\min}$ needed to evaluate the NMO velocity and other attributes associated with the traveltime minimum. It should be emphasized that p_P and p_S corresponding to both zero offset and the traveltime minimum are obtained without using the slowness projection on the interface ($p_{\rm int}$).

In Appendix C we give an explicit solution of equation (12) for isotropic media and demonstrate that the traveltime minimum exists only if

$$\tan\phi \le \frac{2\gamma}{\gamma^2 - 1}\,, \tag{13}$$

where $\gamma \equiv V_P/V_S$, and V_P and V_S are the velocities of the P and S-waves, respectively. For a typical $\gamma = 2$, the moveout curve of the PS-wave has a minimum for reflector dips up to 53°. The limit in equation (13) is not exact if the medium is anisotropic, but it still provides a good approximation for small and moderate values of the anisotropic coefficients.

NMO velocity.—Although the CMP traveltime of converted waves from a dipping reflector is not an even function of source-receiver offset, the moveout curve near the traveltime minimum (if it does exist) can still be described by normal-moveout velocity defined in the same way as that for pure modes:

$$V_{\rm nmo}^2 = \left\{ \frac{1}{2}\,\frac{d^2(t^2)}{dx^2}\,\bigg|_{x_{\min}} \right\}^{-1}\,. \tag{14}$$

Expressing both the traveltime and source-receiver offset through the slowness components and using equation (10) for the moveout slope, we obtain NMO velocity in the following form (Appendix C):

$$V_{{\rm nmo},PS}^2 = \left.\frac{4\,(q_P''\,A_S^2 \,+\, q_S''\,A_P^2)}{(A_P + A_S)^2\,[\,p_P\,(q_P' + q_S') - (q_P + q_S)]}\right|_{p_P^{\min}}\,, \tag{15}$$

where

$$A_P = 1 + q'_P \tan\phi\,, \qquad A_S = 1 + q'_S \tan\phi\,; \tag{16}$$

the parameter $p_P^{\min}$ corresponding to the traveltime minimum is determined from equation (12).

For pure (nonconverted) modes, at the moveout minimum $q_P = q_S$, $q'_P = q'_S$, $q''_P = q''_S$, $A_P = A_S$, and equation (15) reduces to the 2-D NMO equation of Tsvankin (1995) rewritten through the ray parameter (horizontal slowness) by Cohen (1998):

$$V^2_{\rm nmo,pure} = \left.\frac{q''}{pq' - q}\right|_{p^{\min}=p(\phi)} = \frac{V(\phi)}{\cos\phi}\,\frac{\sqrt{1 + \frac{1}{V(\phi)}\frac{d^2V}{d\theta^2}|_{\theta=\phi}}}{1 - \frac{\tan\phi}{V(\phi)}\frac{dV}{d\theta}|_{\theta=\phi}}\,, \tag{17}$$

where $q' \equiv dq/dp$, $q'' \equiv d^2q/dp^2$, $V(\theta)$ is phase velocity as a function of phase angle with vertical, and $p(\phi)$ is the horizontal projection of the slowness vector orthogonal to the reflector. It should be mentioned that reflection-point dispersal in a CMP gather, properly treated in our approach, was not accounted for by Tsvankin (1995). In agreement with Hubral and Krey (1980), the identical result of the two derivations indicates that reflection-point dispersal has no influence on NMO velocity for pure-mode reflections.

For a horizontal reflector ($\phi = 0$), the slowness $p_P^{\min}$ vanishes, and the parameters $A_P = A_S = 1$ [equation (16)]. Hence, equation (15) becomes simply

$$V^2_{{\rm nmo},PS}(\phi = 0) = -\left.\frac{q''_P + q''_S}{q_P + q_S}\right|_{p_P^{\min}=0}. \tag{18}$$

The squared pure-mode NMO velocity [equation (17)] from a horizontal reflector is equal to $(-q''/q)|_{p=0}$, while the traveltime along each of the legs of the PS-wave minimum-traveltime ray (which in general are not vertical) can be written as $t_{{\rm min},P} = z_{\rm CMP}\, q_P$ and $t_{{\rm min},S} = z_{\rm CMP}\, q_S$ [equation (A-16)]. Therefore, equation (18) can be expressed through the NMO velocities of the P- and S-waves as

$$(t_{{\rm min},P} + t_{{\rm min},S})\, V^2_{{\rm nmo},PS} = t_{{\rm min},P}\, V^2_{{\rm nmo},P} + t_{{\rm min},S}\, V^2_{{\rm nmo},S}\,. \tag{19}$$

Since $2t_{{\rm min},P}$ and $2t_{{\rm min},S}$ are the zero-offset reflection traveltimes of the pure P- and S-waves, respectively, equation (19) is the generalization of the VTI relationship (5)

for media without up-down symmetry (i.e., without a horizontal symmetry plane). If the horizontal plane is a plane of symmetry, then the P- and S rays corresponding to the vertical slowness vector are vertical, and equations (19) and (5) become identical.

Other attributes of the traveltime minimum.—Another potentially useful attribute of PS moveout is the offset $x_{\min}$ of the traveltime minimum (for pure modes, $x_{\min}$ always equals zero). Since $x_{\min}$ contains the generally unknown reflector depth z_{CMP}, it is convenient to normalize it by the minimum traveltime $t_{\min}$. Using equations (7) and (8) and taking into account that at the traveltime minimum $p_P = p_S = p_P^{\min}$ [equation (11)], we find

$$\frac{x_{\min}}{t_{\min}} = \left. \frac{q'_P - q'_S}{q_P + q_S - p_P(q'_P + q'_S)} \right|_{p_P^{\min}} . \tag{20}$$

By recording reflection moveout of a converted mode for a range of CMP locations in the dip plane of the reflector, we can also obtain the derivative of $t_{\min}$ with respect to the CMP coordinate $y_{\mathrm{CMP}} = z_{\mathrm{CMP}}/\tan\phi$. In the pure-mode case, the spatial derivative of the minimum (zero-offset) traveltime determines the slope of reflections on the zero-offset (stacked) section and is equal to the ray parameter (horizontal slowness) of the zero-offset ray. For converted waves, $dt_{\min}/dy_{\mathrm{CMP}}$ does not have such a simple interpretation, but it can still provide useful information about the medium parameters. From equations (7) and (8) it follows that

$$\frac{dt_{\min}}{dy_{\mathrm{CMP}}} = \tan\phi \left. \frac{q_P + q_S - p_P(q'_P + q'_S)}{1 + \frac{1}{2}\tan\phi\,(q'_P + q'_S)} \right|_{p_P^{\min}} . \tag{21}$$

The spatial derivative $dx_{\min}/dy_{\mathrm{CMP}}$ can be expressed as a combination of $x_{\min}/t_{\min}$ [equation (20)] and $dt_{\min}/dy_{\mathrm{CMP}}$ [equation (21)] and, therefore, does not yield an independent equation for the medium parameters.

Since the attributes described above already provide an overdetermined system of equations, we did not use some other potential attributes, such as the ratio of $t_{\min}$ and the P-wave zero-offset traveltime $t_{P0}(\phi)$ at a fixed CMP location.

APPLICATION TO VERTICAL TRANSVERSE ISOTROPY

Analytic developments in the previous section are completely general and can be used in a symmetry plane of any anisotropic medium with arbitrary strength of velocity anisotropy. Here, we apply these results to parameter estimation in a transversely isotropic layer with a vertical symmetry axis (VTI media). Note that in VTI models each vertical plane is a plane of mirror symmetry, and our 2-D formalism is valid for any azimuthal orientation of the reflector (that is no longer the case if the symmetry axis is *tilted*).

To gain analytic insight into the influence of anisotropy on reflection traveltimes of the PS-wave, we employ the weak-anisotropy approximation. Then, we devise an algorithm for joint inversion of P and PS data in VTI media based on the exact equations for the moveout attributes. The results below can be directly adapted for the vertical symmetry planes of orthorhombic media by replacing Thomsen parameters with the notation introduced in Tsvankin (1997).

Weak-anisotropy approximation for PS moveout

The weak-anisotropy approximation is a convenient tool for obtaining simple relationships between the reflection moveout of converted waves and parameters of VTI media. For weakly anisotropic models with small (compared to unity) Thomsen's (1986) parameters ϵ and δ, CMP traveltime and source-receiver offset of the PS-wave can be derived as explicit functions of the projection of the slowness vector on the reflector $p_{\rm int}$ [Appendix D, equations (D-11), (D-13)–(D-15)]. The results of Appendix D make it possible to generate the reflection moveout of converted waves for weakly anisotropic VTI media without doing ray tracing or even solving the Christoffel equation.

Despite the explicit form of the weak-anisotropy approximations in Appendix

D, they are rather lengthy and do not provide an easy insight into the influence of anisotropy on the PS reflection moveout. Below we give concise expressions for the moveout attributes discussed above by linearizing the exact equations in the anisotropic parameters.

Slope of the moveout curve.—The weak-anisotropy approximation for the slope of the traveltime curve at zero offset is obtained in Appendix D as [equation (D-23)]

$$\left.\frac{dt}{dx}\right|_{x=0} = \frac{\sin\phi}{2\,V_{P0}\,(1+\gamma)}\,\Big[(1-\gamma^2)+4\gamma\,(\sigma-\delta)\Big] + \frac{\sin^3\phi}{2\,V_{P0}\,\gamma\,(1+\gamma)}\,\Big[\delta\gamma\,(1+\gamma)-\sigma\,(\gamma^3+9\gamma^2+8)\Big] + \frac{\sin^5\phi}{2\,V_{P0}\,\gamma^2\,(1+\gamma)}\,\sigma\,(\gamma^4+5\gamma^3+5\gamma+1)\,, \tag{22}$$

where $\gamma \equiv V_{P0}/V_{S0}$. It is interesting that the higher-order terms in $\sin\phi$ ($\sin^3\phi$ and $\sin^5\phi$) appear only due to the influence of anisotropy. For isotropic media, the exact value of the moveout slope is simply

$$\left.\frac{dt}{dx}\right|_{x=0} (\delta=\sigma=0) \;=\; \frac{\sin\phi\,(1-\gamma)}{2\,V_{P0}}\,. \tag{23}$$

Equation (23) shows that in isotropic models the PS traveltime from a dipping reflector always *decreases* with offset at $x = 0$ ($\gamma > 1$), and the moveout minimum should be recorded at positive x corresponding to the P-wave leg located downdip from the reflection point. In the presence of anisotropy, however, it may happen that $(dt/dx)|_{x=0} > 0$, and the traveltime minimum moves into the negative offset range (where the P-leg is located updip from the reflection point). Indeed, if $\sigma > 0$ and relatively large so that $\sigma - \delta$ is on the order of 0.5, which is quite feasible for such VTI formations as shales, and $\gamma < 2.4$, the leading ($\sin\phi$) term in equation (22) has a positive sign. If the dip is mild, and the influence of the higher-order terms in $\sin\phi$ is small, the zero-offset moveout slope as a whole is greater than zero. For steeper dips, the $\sin^3\phi$-term becomes increasingly dominant and eventually reverses the sign of $(dt/dx)|_{x=0}$. This conclusion is confirmed by the numerical results in Fig. 2 (for

$\phi = 10°$) and Fig. 4b, showing that in VTI media $(dt/dx)|_{x=0}$ may be positive at mild dips, and the PS traveltime reaches a minimum at small negative x.

To explain this unusual phenomenon, recall that for positive σ the SV-wave velocity increases away from vertical up to about 45° [see equation (D-2)]. In this case, although the shear-wave leg for $x < 0$ is longer than at zero offset, the S-wave traveltime does not increase with $|x|$ nearly as fast as in isotropic media because the corresponding group velocity becomes higher. As a result, the overall traveltime of the PS-wave may decrease over a certain range of negative offsets away from $x = 0$.

The deviation of equation (22) from the exact solution is insignificant for moderately anisotropic media (Fig. 4a) and becomes noticeable only when ϵ reaches 0.25-0.3 (Fig. 4b). Note that the model from Fig. 4b has a large $\sigma \approx 0.7$, and the zero-offset moveout slope is positive for dips ranging from 0° to about 17°. The weak-anisotropy approximation correctly reproduces this trend of the exact function in Fig. 4b, but overstates the initial increase in $(dt/dx)|_{x=0}$ with dip.

In the inversion procedure described below, we express reflector dip ϕ through the absolute value of the ray parameter (horizontal slowness) of the pure P-wave reflection recorded at zero offset ($p_{P0} = |p_{P,\text{pure}}(x = 0)|$). Unlike reflector dip, p_{P0} can be found from surface data by measuring reflection slopes on zero-offset (stacked) P-wave sections (e.g., Alkhalifah and Tsvankin 1995). Neglecting the cubic and higher-order terms in $\sin\phi$, the P-wave ray parameter can be written as

$$p_{P0} = \frac{\sin\phi}{V_P(\phi)} \approx \frac{\sin\phi}{V_{P0}}\,. \tag{24}$$

If we retain only the leading term in $\sin\phi$ in equation (22), the P-wave ray parameter can be substituted in its approximate form [equation (24)] yielding

$$\left.\frac{dt}{dx}\right|_{x=0} = \frac{p_{P0}}{2\,(1+\gamma)}\,\left[(1-\gamma^2) + 4\gamma\,(\sigma-\delta)\right] + \ \ldots\,. \tag{25}$$

For a typical value of $\gamma = 2$, the coefficient multiplied with the anisotropic term $\sigma - \delta$ is almost three times greater than the isotropic term $1 - \gamma^2$. Therefore, we can expect

that $(dt/dx)|_{x=0}$, obtained as a function of p_{P0}, can provide reliable information about the anisotropic parameters δ and σ (or δ and ϵ). Note that in the inversion algorithm discussed below we use the exact representations for both the parameter p_{P0} and the moveout slope at zero offset.

Attributes of the traveltime minimum.—As discussed above, traveltime curves of the PS-wave have a minimum only for small and moderate reflector dips. Hence, it is convenient to use simplified "mild-dip" approximations for the attributes of the traveltime minimum, in which all terms containing the cubic and higher powers of $\sin\phi$ have been dropped.

The weak-anisotropy, mild-dip approximation for converted-wave NMO velocity is derived in Appendix D as

$$V_{\mathrm{nmo},PS}^{-2}(p_{P0}) = V_{\mathrm{nmo},PS}^{-2}(0) - \frac{p_{P0}^2}{8\gamma}\left(3\gamma^4 - 2\gamma^3 + 6\gamma^2 - 2\gamma + 3\right) - \frac{p_{P0}^2(\gamma-1)}{2\gamma(\gamma+1)}\left[6\sigma(\gamma+1)^2 - (\sigma-\delta)\gamma(3\gamma^2 - 2\gamma + 3)\right]. \quad (26)$$

The parameter σ was introduced in equation (4), and $V_{\mathrm{nmo},PS}(0)$ is the weak-anisotropy approximation for the NMO velocity from a horizontal reflector:

$$V_{\mathrm{nmo},PS}^{-2}(0) = \frac{1}{V_{P0}V_{S0}}\left[1 - \frac{2(\sigma+\delta\gamma)}{1+\gamma}\right]. \quad (27)$$

To estimate the contribution of the anisotropic parameters to the dip dependence of NMO velocity, we rewrite equations (26) and (27) for a typical velocity ratio $\gamma = 2$:

$$V_{\mathrm{nmo},PS}^{-2}(p_{P0}, \gamma = 2) = \frac{1}{V_{P0}V_{S0}}\left[1 - 1.3(\delta + 0.5\sigma)\right] - 3.4p_{P0}^2 - p_{P0}^2(2.7\sigma + 1.8\delta). \quad (28)$$

Equation (28) shows that for positive values of σ, commonly observed in VTI formations, anisotropy amplifies the increase in the NMO velocity with dip (usually $\sigma > \delta$). The anisotropic dip-dependent term $[p_{P0}^2(2.7\sigma + 1.8\delta)]$ provides an equation for σ and δ with comparable weights for both parameters. However, for a typical $\sigma = 0.4 - 0.5$ the magnitude of this term can reach only 35-40% of the isotropic one $(3.4p_{P0}^2)$, and the dip-dependence of NMO velocity as a whole is not highly sensitive

to the anisotropic parameters. Our numerical tests show that the contribution of the anisotropic parameters to the exact NMO velocity is even somewhat smaller than predicted by equation (26).

The accuracy of the weak-anisotropy approximation (26) is illustrated by Fig. 5. Since we retained just the leading term in ϕ and p_{P0}, the approximation deviates from the exact solution with increasing dip. Despite this deterioration in accuracy, our approximations correctly reproduce the trend of the dip dependence of moveout attributes in the most important regime of moderate dips ($\phi < 35-40^\circ$). For steeper dips, the traveltime minimum either does not exist at all or corresponds to unusually large source-receiver offsets seldom acquired in practice. Comparison of Figs. 5a and 5b also shows that the error is higher for more "anelliptical" models with larger values of σ. It should be emphasized that the main value of equation (26) and other approximations in this section is in providing analytic insight into the behavior of various moveout attributes.

The leading dip term in the weak-anisotropy approximation for the normalized offset $x_{\min}/t_{\min}$ [equation (D-33)] has the following form:

$$\frac{x_{\min}}{t_{\min}} = \frac{p_{P0}\, V_{P0}^2}{2\gamma}\left[(\gamma-1)+2(\delta\gamma-\sigma)\right]. \tag{29}$$

For $\gamma = 2$, the multiplier of the anisotropic term in equation (29) is twice as large as the isotropic term, and we can expect $x_{\min}/t_{\min}$ to be quite sensitive to the parameters δ and σ.

The approximate spatial derivative of the minimum traveltime ($dt_{\min}/dy_{\mathrm{CMP}}$) is found in Appendix D as

$$\frac{dt_{\min}}{dy_{\mathrm{CMP}}} = p_{P0}\,(1+\gamma). \tag{30}$$

Clearly, equation (30) is purely isotropic and gives only redundant information about the ratio of the vertical velocities, which can be determined in a conventional way using the vertical traveltimes [equation (6)].

On the whole, the analytic approximations presented above indicate that dip moveout of the converted PS-wave can be efficiently used in anisotropic parameter estimation. This conclusion is supported below by numerical inversion based on the exact equations for the moveout attributes.

Parameter estimation in VTI media using dip moveout of PS-waves

As suggested by the form of the weak-anisotropy approximations, the addition of the dip moveout of PS-waves to P-wave data can help to stabilize parameter estimation in VTI media. Thus, the data used in the inversion for V_{P0}, V_{S0}, ϵ, δ include the moveout of P and PS-waves from a horizontal reflector and on the dip line of a dipping reflector. (The horizontal and dipping interface are embedded in the same homogeneous VTI layer.) Also, we assume that the P-wave ray parameter for the dipping event ($p_{_{P0}}$) was determined from the slope of the P-wave reflection on the zero-offset (stacked) section. The vertical traveltimes and NMO velocities of the P- and PS-waves from a horizontal reflector allow us to obtain the V_{P0}/V_{S0} ratio and the NMO velocity of the SV-wave [see equation (5)]. By using the P-wave NMO velocity for a dipping event [equation (17)], we include an equation for the anisotropic parameter η since $V_{\mathrm{nmo},P}(p_{_{P0}}) = f[V_{\mathrm{nmo},P}(0), \eta]$. Although this information [equations (1), (2), (3), and (6)] is sufficient for determination of all four unknowns, the solution of this inverse problem, as discussed in the introduction, suffers from instability; this is further confirmed by a numerical test below. The dip-moveout attributes of the PS-wave allow us to build an overdetermined system of equations needed to obtain more accurate estimates of the vertical velocities and anisotropic parameters.

Recovery of the moveout attributes of the PS-wave.—An important practical issue is how to determine the attributes associated with the PS-wave traveltime minimum (t_{min}, x_{min}, and $V_{\mathrm{nmo},PS}$) from moveout data. Since the first derivative of the PS-wave traveltime curve (dt/dx) goes to zero at x_{min}, we suggest approximating

the PS moveout with a hyperbola centered at the traveltime minimum:

$$t^2(x) = t^2_{\min} + \frac{(x - x_{\min})^2}{V^2_{\mathrm{nmo},PS}}\,. \tag{31}$$

A typical example illustrating the application of a shifted hyperbola to the recovery of the moveout attributes is shown in Fig. 6. Note that the exact PS-wave traveltimes $t(x)$ (solid) are generally asymmetric with respect to $x_{\min}$ due to the presence of a term cubic in $(x - x_{\min})$, which is not included in equation (31). This, however, does not prevent the hyperbola (31) (dashed) from giving the correct position of the moveout apex $(x_{\min}, t_{\min})$ and an accurate value of the NMO velocity. The errors in the estimates of V_{nmo} and $x_{\min}/t_{\min}$ [compared to the exact values given by equations (15) and (20)] are only 1.1% and 0.05%, respectively. The high accuracy achieved for the model from Fig. 6 was ensured by having an approximately equal range of offsets on each side of the apex of the moveout curve, which mitigates the influence of the cubic moveout term. If the traveltime minimum is substantially shifted with respect to zero offset, it may be necessary either to mute out a certain range of offsets (making the fitting interval more symmetric with respect to $x_{\min}$) or add the cubic term in $x - x_{\min}$ to the moveout equation. To obtain the slope of the moveout curve at $x = 0$, we approximate the traveltimes at small source-receiver offsets with a straight line or a quadratic, depending on the moveout curvature.

In most field-data applications, the moveout curve of the PS-wave has to be found by means of semblance velocity analysis based on equation (31). Since the results of semblance scan may be influenced by the offset-dependent amplitude and waveform of the reflection event, as well as the offset coverage, we generated synthetic seismograms of the PS-wave using dynamic ray tracing (Fig. 7). For dips up to 40-45°, the amplitude of the converted wave goes to zero at relatively small offsets close to the traveltime minimum (e.g., at zero offset for a horizontal reflector), which may cause complications in the semblance analysis and reconstruction of the moveout curve. Although the low amplitudes are observed over a narrow range of offsets, the polarity

change in the wavelet may cause errors in calculating the semblance along shifted hyperbolas (31). To make an appropriate correction, we suggest computing the RMS amplitude for each seismogram within the time window used in the semblance search and identify the minimum-amplitude trace. Then, prior to calculating the semblance, one has to reverse the polarity of all traces at offsets larger than that of the moveout minimum. Note that if the dip exceeds 30°, the amplitude minimum moves towards longer offsets and does not interfere with determination of the zero-offset moveout slope.

Inversion procedure.—Our inversion algorithm is organized in the following way. Using the relationship between the NMO velocities for horizontal events [equation (5)], we determine the SV-wave NMO velocity [equation (3)] from P and PS data. The vertical-velocity ratio $\gamma \equiv V_{P0}/V_{S0}$ is obtained from the vertical traveltimes of P- and PS-waves. Then, for a given value of δ, we find the other three parameters [see equations (1), (3), (4), (6)]:

$$V_{P0} = \frac{V_{\mathrm{nmo},P}}{\sqrt{1+2\delta}}\,, \tag{32}$$

$$V_{S0} = \frac{V_{P0}}{\gamma}\,, \tag{33}$$

$$\epsilon = \frac{\sigma}{\gamma^2} + \delta \quad [\sigma = \frac{1}{2}\left(\frac{V^2_{\mathrm{nmo},SV}}{V^2_{S0}} - 1\right)]\,. \tag{34}$$

The last step is to use the P-wave NMO velocity $V_{\mathrm{nmo},P}(p_{P0})$ and PS-wave moveout attributes for the same dipping reflector to invert for the remaining unknown parameter δ. If the PS traveltime does have a minimum on the CMP gather, δ is found by minimizing the following objective function:

$$\mathcal{F}^{(1)}_{P,SV} = \left[\frac{V_{\mathrm{nmo},P}(p_{P0}) - V^{\mathrm{meas}}_{\mathrm{nmo},P}(p_{P0})}{V^{\mathrm{meas}}_{\mathrm{nmo},P}(p_{P0})}\right]^2 + \left[\frac{(dt/dx|_{x=0}) - (dt/dx|_{x=0})^{\mathrm{meas}}}{(dt/dx|_{x=0})^{\mathrm{meas}}}\right]^2$$
$$+ \left[\frac{(x_{\min}/t_{\min}) - (x_{\min}/t_{\min})^{\mathrm{meas}}}{(x_{\min}/t_{\min})^{\mathrm{meas}}}\right]^2 + \left[\frac{V_{\mathrm{nmo},PS}(p_{P0}) - V^{\mathrm{meas}}_{\mathrm{nmo},PS}(p_{P0})}{V^{\mathrm{meas}}_{\mathrm{nmo},PS}(p_{P0})}\right]^2 . \tag{35}$$

Here the superscript "meas" denotes the values measured from the data, while the quantities without the subscript are computed from the exact equations (17), (15), (20) and (10). Essentially, the objective function (35) represents an overdetermined system of four nonlinear equations for the single unknown parameter δ.

For PS traveltime curves without a minimum, the objective function contains only one PS moveout attribute – the slope of the moveout curve at $x = 0$ [equation (10)]:

$$\mathcal{F}^{(2)}_{P,SV} = \left[\frac{V_{\mathrm{nmo},P}(p_{P0}) - V^{\mathrm{meas}}_{\mathrm{nmo},P}(p_{P0})}{V^{\mathrm{meas}}_{\mathrm{nmo},P}(p_{P0})}\right]^2 + \left[\frac{(dt/dx|_{x=0}) - (dt/dx|_{x=0})^{\mathrm{meas}}}{(dt/dx|_{x=0})^{\mathrm{meas}}}\right]^2 . \quad (36)$$

Numerical test.—A numerical example of the joint inversion of P and PS data based on equations (32)–(36) is displayed in Fig. 8. All input parameters were computed from the exact equations and contaminated by Gaussian noise with standard deviations simulating realistic errors in data measurements. The inversion results (dots) were obtained for 200 realizations of the input data set distorted by noise.

To generate the top pair of plots (Figs. 8a,b), we excluded the terms involving the moveout attributes of the PS-wave from the objective function (35). As expected, the parameter η can be accurately estimated from the P-wave NMO velocity of the dipping event, and the ϵ and δ points in Fig. 8a are close to the line corresponding to the correct value of η. However, the inversion results for V_{P0}, V_{S0}, ϵ, and δ exhibit significant scatter indicative of high sensitivity to errors in the input data. The standard deviations in all four parameters are too significant for this algorithm to be used in practice (8.6% for V_{P0} and V_{S0}, 0.13 for ϵ and 0.09 for δ).

Minimization using the full objective function (35) (including the dip-moveout attributes of the PS-wave) leads to a dramatic reduction in the scatter for all medium parameters, with standard deviations of only 2.5% for V_{P0} and V_{S0}, 0.03 for ϵ and 0.02 for δ (Figs. 8c,d). Clearly, the dip-moveout attributes of the PS-wave allowed us to overcome the problem of error amplification in the transition from η to the vertical velocities and anisotropic coefficients.

Figs. 8a-d correspond to a relatively mild reflector dip of 30°. As the dip reaches

50°, the CMP traveltime of the PS-wave no longer has a minimum, and we need to use the second form of the objective function [equation (36)] that includes only the slope of the PS moveout curve at zero offset (Figs. 8e,f). Since the moveout attributes of both P and PS-waves become more sensitive to the anisotropic parameters with increasing dip, the inversion results for the $\phi = 50°$ are even better than those for $\phi = 30°$ (the standard deviations are 1.2% for V_{P0} and V_{S0}, and 0.01 for ϵ and δ).

DISCUSSION AND CONCLUSIONS

To determine the vertical velocity and the anisotropic parameters of VTI media from surface data, reflection moveout of P-waves can be combined with S-wave traveltimes. In many cases, a more practical option than to explicitly conduct shear-wave surveys is to supplement P-wave moveout with converted-wave data. Analysis of the kinematic inverse problem shows that it is necessary to include PS (PSV) traveltimes not just from a horizontal reflector, but also from at least one dipping interface.

Moveout of PS-waves in CMP geometry generally is asymmetric with respect to zero offset, with the position of the traveltime minimum strongly dependent on reflector dip and anisotropic parameters. As in isotropic media, the minimum usually is recorded at "positive" offsets corresponding to the P-wave leg located *downdip* from the reflection point. For VTI media with large positive values of the parameter $\sigma = 0.5 - 0.8$ and mild reflector dips, however, the traveltime reaches its minimum at *negative* offsets. Further increase in σ leads to the development of cusps on the wavefront of the PS-wave and multivalued PS moveout function for a certain range of offsets (e.g., Tsvankin and Thomsen, 1994); treatment of such models is outside of the scope of this paper.

For relatively mild dips up to 30-40°, the minimum is observed at moderate offsets and can be recorded in a conventional-length CMP gather. In this case, PS traveltimes can be used to recover moveout attributes associated with the traveltime

minimum $t_{\min}(x_{\min})$, such as the normal-moveout velocity (defined by analogy with pure modes) and the ratio $x_{\min}/t_{\min}$. These attributes can be obtained from reflection data by approximating PS-moveout with a *shifted* hyperbola centered at the offset $x_{\min}$. If reflector dip exceeds $40-50^\circ$, the traveltime minimum either does not exist at all or cannot be captured on conventional spreads (limited by 1.5–2 distances between the CMP and the reflector). For these traveltime functions, monotonically decreasing with offset, a natural attribute is the slope of the moveout curve at the CMP location.

To apply the PS-wave moveout attributes in anisotropic parameter estimation, we developed an analytic treatment of dip moveout of converted waves valid in a vertical symmetry plane of an anisotropic layer with arbitrary strength of anisotropy (e.g., the model can be orthorhombic). Parametric representation of the PS traveltime and CMP offset in terms of the slowness vector yields a concise description of reflection moveout involving the vertical and horizontal slowness components of the P- and S-waves. Although the computation of the source-receiver offset and corresponding traveltime involves solving the Christoffel equation, our expression can be used to generate the CMP moveout curve without time-consuming two-point ray tracing.

We also proved that the slope of any moveout curve in CMP geometry is always equal to one half of the difference between the ray parameters (horizontal slownesses) evaluated for the incident and reflected ray at the source and receiver locations. This simple result, which remains valid for symmetry planes in inhomogeneous anisotropic media, was combined with the parametric traveltime-offset relationships to derive closed-form expressions for all moveout attributes described above.

These analytic developments provide a basis for a joint inversion of P and PS data in VTI media. The weak-anisotropy approximation allowed us to find explicit expressions for the traveltime and offset of the PS-wave and study the dependence of the moveout attributes on the anisotropic parameters. The attributes that proved to be mostly sensitive to the anisotropy are the normalized offset $x_{\min}/t_{\min}$ and the

slope of the $t(x)$ curve at zero offset, while the contribution of anisotropy to the dip-dependence of the PS-wave NMO velocity is somewhat smaller.

Our inversion algorithm is designed to recover the medium parameters (the P- and S-wave vertical velocities V_{P0} and V_{S0} and the anisotropic coefficients ϵ and δ) using the NMO velocities and vertical traveltimes of the P and PS-waves from a horizontal reflector, P-wave NMO velocity from a dipping reflector, and PS moveout attributes associated with the same dipping event. Although the number of equations is sufficient to obtain all unknowns even without the dip-moveout attributes of the PS-wave, such an inversion procedure is rather unstable. While the parameter $\eta \approx \epsilon - \delta$ is well-constrained by the dip dependence of P-wave moveout, small errors in η propagate with considerable amplification into the vertical velocities and anisotropic parameters. The addition of the PS moveout attributes to the input data leads to a significant improvement in the stability of the inversion procedure. It is interesting that the disappearance of the PS traveltime minimum at steep dips does not impair the stability of the parameter estimation. On the contrary, the accuracy in all inverted parameters increases with dip due to the higher sensitivity of the dip-moveout attributes to the anisotropy.

We showed that combining P and PS reflection traveltimes in moveout inversion yields all parameters of VTI media needed for *depth* imaging of P, SV, or PS-waves. Therefore, an important future application of our method is in building velocity models for P-wave prestack or poststack depth migration. However, the algorithm presented here will not be able to handle realistic subsurface models unless it accounts for vertical (and maybe lateral) heterogeneity. Such an extension is discussed in a sequel paper (to be presented at the 69th SEG Meeting in Houston) devoted to the determination of the PS-moveout attributes in layered anisotropic media.

Processing of converted waves in VTI media is also impossible without knowledge of both vertical velocities and the parameters ϵ and δ. Although our inversion has to be performed on common-midpoint gathers, reflection-point dispersal makes it

necessary to re-sort the data into common-reflection-point (CRP) gathers prior to stacking. This operation proved to be sensitive to the anisotropic coefficients of VTI media and vertical velocities (Rommel 1997) and, therefore, has to be preceded by parameter estimation. In principle, it is possible to repeat the inversion procedure on CRP gathers to refine the estimates of the medium parameters, but such an algorithm was not implemented in this work. An alternative way to generate a zero-offset section for converted waves is the transformation to zero offset (TZO), which also requires an accurate VTI model (Anderson 1996). In addition, our analytic expressions for the converted-wave reflection moveout can be used to extend dip-moveout processing algorithms to PS-modes in anisotropic media.

Due to the kinematic equivalence between the symmetry planes of orthorhombic and VTI media, our results remain valid for CMP reflections in both vertical symmetry planes of models with orthorhombic symmetry (Tsvankin 1997). The only change required in our equations is the replacement of ϵ, δ, and the shear-wave vertical velocity V_{S0} with the appropriate set of parameters introduced by Tsvankin (1997).

ACKNOWLEDGEMENTS

We are grateful to James Gaiser (Western), Leon Thomsen (Amoco) and members of the A(nisotropy)-Team of the Center for Wave Phenomena (CWP) at CSM for helpful suggestions and to Ken Larner (CSM) for his review of the manuscript. The support for this work was provided by the members of the Consortium Project on Seismic Inverse Methods for Complex Structures at CWP and by the United States Department of Energy. I. Tsvankin was also supported by the Shell Faculty Career Initiation Grant.

APPENDIX A–CONVERTED-WAVE MOVEOUT FROM DIPPING REFLECTORS

The objective of this Appendix is to derive a parameteric representation of reflection moveout of a PS-wave recorded in CMP geometry in the dip direction of a plane reflector. It is assumed that the incidence plane also represents a symmetry plane of the (anisotropic) medium, so both rays and the corresponding phase-velocity vectors of the reflected waves are confined to the incidence plane; also, the P-wave generates only one converted mode polarized in the vertical plane. Without losing generality, we assume that the P-leg is located downdip from the reflection point (Fig. 3). Then the reflection traveltime can be written as

$$t = t_P + t_S = \frac{z_r}{g_P \cos\theta_P^{\rm gr}} + \frac{z_r}{g_S \cos\theta_S^{\rm gr}}\,, \tag{A-1}$$

where $\theta_P^{\rm gr}$ and $\theta_S^{\rm gr}$ are the group angles with vertical for the P and S segments of the reflected ray (Fig. 3), g_P and g_S are the corresponding group velocities, and z_r is the depth of the reflection point. The source-receiver offset in terms of the group angles is given by

$$x = x_P + x_S = z_r\,(\tan\theta_P^{\rm gr} + \tan\theta_S^{\rm gr})\,. \tag{A-2}$$

The angle $\theta_S^{\rm gr}$ in equation (A-1) and below is considered negative if the S-ray is tilted downdip from vertical. Introducing the reflector depth beneath the common midpoint ($z_{\rm CMP}$) instead of z_r yields

$$z_{\rm CMP} = z_r\,[1 + \frac{1}{2}\tan\phi\,(\tan\theta_P^{\rm gr} - \tan\theta_S^{\rm gr})]\,, \tag{A-3}$$

where ϕ is reflector dip. Substituting $z_{\rm CMP}$ [equation (A-3)] into equations (A-1) and (A-2), we find

$$t = z_{\rm CMP}\,\frac{N}{D} \tag{A-4}$$

and

$$x = z_{\rm CMP}\,\frac{N_x}{D}\,, \tag{A-5}$$

where

$$N = \frac{1}{g_P\,\cos\theta_P^{\rm gr}} + \frac{1}{g_S\,\cos\theta_S^{\rm gr}}\,, \tag{A-6}$$

$$D = 1 + \frac{1}{2}\tan\phi\,(\tan\theta_P^{\rm gr} - \tan\theta_S^{\rm gr})\,, \tag{A-7}$$

$$N_x = \tan\theta_P^{\rm gr} + \tan\theta_S^{\rm gr}\,. \tag{A-8}$$

To satisfy Snell's law, the P and S-waves should have the same projection of the slowness vector (ray parameter) on the interface at the reflection point. Hence, this projection ($p_{\rm int}$; the subscript stands for the interface) can be conveniently used to build a parametric representation of the CMP traveltime for the converted wave. Hereafter, we assume that $p_{\rm int}$ is the "updip" projection, which corresponds to the upgoing S-wave and downgoing P-wave.

If the medium is isotropic, the group angles $\theta_P^{\rm gr}$ and $\theta_S^{\rm gr}$ are equal to the corresponding phase angles and can be easily expressed through $p_{\rm int}$ (taken to be non-negative), reflector dip ϕ, and the velocities of the P- and S-waves (V_P and V_S):

$$\sin\theta_P^{\rm gr} = p_{\rm int}V_P\cos\phi + \sqrt{1 - p_{\rm int}^2V_P^2}\,\sin\phi\,, \tag{A-9}$$

$$\cos\theta_P^{\rm gr} = \sqrt{1 - p_{\rm int}^2V_P^2}\,\cos\phi - p_{\rm int}V_P\sin\phi\,, \tag{A-10}$$

$$\sin\theta_S^{\rm gr} = p_{\rm int}V_S\cos\phi - \sqrt{1 - p_{\rm int}^2V_S^2}\,\sin\phi\,, \tag{A-11}$$

$$\cos\theta_S^{\rm gr} = \sqrt{1 - p_{\rm int}^2V_S^2}\,\cos\phi + p_{\rm int}V_S\sin\phi\,. \tag{A-12}$$

Substitution of equations (A-9)–(A-12) into equations (A-6)–(A-8) and then (A-4) and (A-5) leads to explicit expressions for the reflection traveltime and source-receiver offset in CMP geometry in terms of the slowness $p_{\rm int}$.

For anisotropic media, the transition from the slowness (ray parameter) $p_{\rm int}$ to the group angles of the reflected waves involves solving the Christoffel equation for the slowness component orthogonal to the reflector. For $P-SV$-waves in a symmetry plane of an anisotropic medium, the Christoffel equation for an unknown slowness component is quartic (it becomes sextic outside the symmetry planes).

Since we may have several reflectors with different dips in the same medium, it is more convenient to express the traveltime curve through the slowness components in the unrotated coordinate system associated with the earth surface. Also, note that the group angles in equations (A-1)–(A-5) are defined with respect to the vertical axis rather than the reflector normal (i.e., the vector normal to the reflector). Introducing the projections of the group-velocity vectors of P- and S-waves on the vertical (x_3, subscript "3") and horizontal (x_1, subscript "1") axes, we obtain the following equivalent form of equations (A-6)–(A-8):

$$N = \frac{1}{g_{P3}} + \frac{1}{g_{S3}}\,, \tag{A-13}$$

$$D = 1 - \frac{1}{2}\tan\phi\,(\frac{g_{P1}}{g_{P3}} + \frac{g_{S1}}{g_{S3}})\,, \tag{A-14}$$

$$N_x = -\frac{g_{P1}}{g_{P3}} + \frac{g_{S1}}{g_{S3}}\,. \tag{A-15}$$

Here the x_3-axis is directed upward, the x_1-axis is in the updip direction, and both group-velocity vectors are assumed to point from the reflector towards the surface. The group-velocity components can be related to the slowness vector in the same (unrotated) coordinate system in the following way (Cohen 1998):

$$g_3 = \frac{1}{q - pq'} \tag{A-16}$$

and

$$g_1 = -g_3 q'\,, \tag{A-17}$$

where q and p are the vertical and horizontal slowness components, respectively, and $q' \equiv dq/dp$. Equations (A-16) and (A-17) allow us to rewrite equations (A-13)–(A-15) as

$$N = q_P - p_P q'_P + q_S - p_S q'_S \,, \tag{A-18}$$

$$D = 1 + \frac{1}{2} \tan\phi \, (q'_P + q'_S) \,, \tag{A-19}$$

$$N_x = q'_P - q'_S \,. \tag{A-20}$$

Here p_P and p_S are the horizontal components of the slowness vector for the P- and S-waves, and $q'_P \equiv dq_P/dp_P$, $q'_S \equiv dq_S/dp_S$. Note that if the P-wave leg is tilted updip from the reflection point, under our convention the value of N_x and source-receiver offset are *negative*.

To generate a CMP gather of the converted PS-wave, we first need to obtain p_P and p_S as functions of the projection of the slowness vector on the reflector ($p_{\rm int}$) by solving the Christoffel equation for the slowness vectors of the P- and S-waves in the rotated coordinate system with one of the axes parallel to the reflecting interface. Then we can find p_P and p_S and use them in equations (A-18)–(A-20), (A-4), and (A-5) to obtain the moveout curve of the converted mode.

APPENDIX B–GENERAL EXPRESSION FOR THE SLOPE OF REFLECTION MOVEOUT

The goal of this appendix is to prove that the apparent slowness (slope) of the CMP moveout curve for any converted or pure reflection is determined by the difference between the ray parameters (slownesses) corresponding to the two legs of the reflected ray. As before, we assume a 2-D model of wave propagation, with the group velocities of the reflected waves confined to the incidence plane. The medium above the reflector, however, is no longer restricted to a single homogeneous layer and may be inhomogeneous and anisotropic (with the incidence plane still being a plane of symmetry).

Suppose the reflected wave represents a converted PS mode recorded in CMP geometry (Fig. B-1). The slope of the moveout curve at any offset x_0 is given by

$$\left.\frac{dt}{dx}\right|_{x_0} = \left.\frac{d(t_P + t_S)}{dx}\right|_{x_0}, \tag{B-1}$$

where t_P is the traveltime along segment S_1O_1 and t_S corresponds to O_1R_1 (Fig. B-1). To relate the moveout slope to the ray parameters of the P- and S-waves, it is convenient to add and subtract from dt/dx the slope of the reflection traveltime $t^{\rm ns}$ along a *non-specular* raypath S_1OR_1. Expressing $t^{\rm ns}$ through the sum of the P and S traveltimes $t_P^{\rm ns}$ and $t_S^{\rm ns}$, we rewrite equation (B-1) in the form

$$\left.\frac{dt}{dx}\right|_{x_0} = \left.\frac{d(t_P^{\rm ns} + t_S^{\rm ns})}{dx}\right|_{x_0} + \left.\frac{d(t_P + t_S - t_P^{\rm ns} - t_S^{\rm ns})}{dx}\right|_{x_0}. \tag{B-2}$$

Since the P- and S-legs of the non-specular raypath originate from the fixed reflection point O, the slope of the corresponding moveout curve can be expressed as

$$\left.\frac{d(t_P^{\rm ns} + t_S^{\rm ns})}{dx}\right|_{x_0} = \left.\frac{d(t_P^{\rm ns} + t_S^{\rm ns})}{d(2h)}\right|_{h_0} = \frac{1}{2}\left[-p_P(-h_0) + p_S(h_0)\right], \tag{B-3}$$

where $h \equiv x/2$, $h_0 \equiv x_0/2$, p_P and p_S are the horizontal slownesses (ray parameters) evaluated at the surface for the P- and S-rays OS and OR, and the horizontal coordinate axis runs updip.

To prove that the remaining (second) term in the right-hand side of equation (B-2) is equal to zero, we consider all possible non-specular reflections with the source-receiver offset $x = S_1R_1$ (Fig. B-1). The traveltimes of these arrivals can be expanded into a Taylor series in the distance $l = OO_1$ between the specular (O_1) and non-specular reflection point. According to Fermat's principle, the minimum traveltime corresponds to the specular reflection, so the term linear in l in this expansion should vanish. Hence, dropping the cubic and higher-order terms in l, we obtain the following relationship between the nonspecular ($t^{\rm ns} = t_P^{\rm ns} + t_S^{\rm ns}$) and specular ($t = t_P + t_S$) traveltimes:

$$t^{\rm ns} = t + \frac{1}{2}\left.\frac{d^2t^{\rm ns}}{dl^2}\right|_{l=0} l^2 + \dots . \tag{B-4}$$

Therefore, the difference between the traveltimes along the raypaths $S_1O_1R_1$ and S_1OR_1 (Fig. B-1) becomes

$$t - t^{\rm ns} = A(x)\, l^2(x)\,, \tag{B-5}$$

where

$$A(x) = -\frac{1}{2}\left.\frac{d^2t^{\rm ns}}{dl^2}\right|_{l=0} . \tag{B-6}$$

Differentiating equation (B-5) with respect to x at $x = x_0$ yields

$$\left.\frac{d(t - t^{\rm ns})}{dx}\right|_{x_0} = \left.\frac{dA(x)}{dx}\, l^2(x)\right|_{l=0} + A(x)\, 2l \left.\frac{dl}{dx}\right|_{l=0} = 0\,. \tag{B-7}$$

Therefore, the slope of the moveout curve can be determined from the non-specular traveltime [equation (B-3)]:

$$\left.\frac{dt}{dx}\right|_{x_0} = \frac{1}{2}\left[-p_P(-h_0) + p_S(h_0)\right] . \tag{B-8}$$

APPENDIX C–NMO VELOCITY FOR CONVERTED-WAVE MOVEOUT

If reflection moveout of a converted wave in a CMP gather does have a minimum $t_{\rm min} = t(x_{\rm min})$, the traveltime near $t_{\rm min}$ can be described by normal-moveout velocity $V_{\rm nmo}$ introduced by analogy with pure modes. To find an analytic expression for $V_{\rm nmo}$, we expand the squared CMP traveltime $t^2(x)$ into a Taylor series near the traveltime minimum:

$$t^2(x) = t^2_{\rm min} \,+\, \left.\frac{d(t^2)}{dx}\right|_{x_{\rm min}} (x - x_{\rm min}) \,+\, \frac{1}{2}\left.\frac{d^2(t^2)}{dx^2}\right|_{x_{\rm min}} (x - x_{\rm min})^2 \,+\, \ldots \qquad \text{(C-1)}$$

The first derivative $d(t^2)/dx$ at $x = x_{\rm min}$ is equal to zero, while the second derivative yields the NMO velocity that governs the traveltime for small $(x - x_{\rm min})$:

$$V^2_{\rm nmo} = \left\{ \frac{1}{2}\left.\frac{d^2(t^2)}{dx^2}\right|_{x_{\rm min}} \right\}^{-1} = \left\{ t\,\frac{d}{dx}\left(\frac{dt}{dx}\right)\Big|_{x_{\rm min}} \right\}^{-1} . \qquad \text{(C-2)}$$

Using the results of Appendix B, the moveout slope dt/dx can be expressed through the difference between the horizontal slownesses of the P- and S-waves:

$$\frac{dt}{dx} = \frac{1}{2}\,(p_S - p_P)\,. \qquad \text{(C-3)}$$

Considering both dt/dx and x as functions of the projection of the slowness vector on the interface ($p_{\rm int}$), we can rewrite equation (C-2) as

$$V^2_{{\rm nmo},PS} = \left\{ \frac{t}{2}\left.\frac{d(p_S - p_P)/dp_{\rm int}}{dx/dp_{\rm int}}\right|_{p^{\rm min}_{\rm int}} \right\}^{-1} , \qquad \text{(C-4)}$$

where $p^{\rm min}_{\rm int}$ corresponds to the traveltime minimum.

To evaluate the derivatives in equation (C-4), $p_{\rm int}$ should be represented through the slownesses of the P- and S-waves using Snell's law:

$$p_{\rm int} = -(p_P \cos\phi + q_P \sin\phi) = p_S \cos\phi + q_S \sin\phi\,. \qquad \text{(C-5)}$$

The P-wave in equations (A-13)–(A-15) is assumed to travel *upward* from the reflector, which explains the minus sign in front of the P-wave term in equation (C-5). Differentiating equation (C-5), we obtain

$$\frac{dp_P}{dp_{\rm int}} = -(\cos\phi + q'_P \sin\phi)^{-1}\,, \tag{C-6}$$

$$\frac{dp_S}{dp_{\rm int}} = (\cos\phi + q'_S \sin\phi)^{-1}\,, \tag{C-7}$$

where, as in equations (A-18)–(A-20), $q'_P \equiv dq_P/dp_P$ and $q'_S \equiv dq_S/dp_S$. Hence,

$$\frac{d(p_S - p_P)}{dp_{\rm int}} = \frac{1}{\cos\phi}\,\left[\frac{1}{1 + q'_P \tan\phi} + \frac{1}{1 + q'_S \tan\phi}\right]. \tag{C-8}$$

The derivative $dx/dp_{\rm int}$ in equation (C-4) can be represented through D and N_x [equations (A-19) and (A-20)] as

$$\frac{dx}{dp_{\rm int}} = z_{\rm CMP}\,\frac{d(N_x/D)}{dp_{\rm int}} = z_{\rm CMP}\,\frac{(dN_x/dp_{\rm int})\,D - (dD/dp_{\rm int})\,N_x}{D^2}\,. \tag{C-9}$$

Using equations (C-6) and (C-7), the derivatives with respect to $p_{\rm int}$ can be expressed through those with respect to p_P or p_S; for instance,

$$\frac{dq_P}{dp_{\rm int}} = -q'_P(\cos\phi + q'_P \sin\phi)^{-1}\,. \tag{C-10}$$

Equation (C-10) and an analogous expression for q_S allow us to obtain the numerator in equation (C-9) in the following form:

$$\frac{dN_x}{dp_{\rm int}}D - \frac{dD}{dp_{\rm int}}N_x = -\,\frac{q''_P\,(1 + q'_S\,\tan\phi)}{\cos\phi + q'_P \sin\phi} - \,\frac{q''_S\,(1 + q'_P\,\tan\phi)}{\cos\phi + q'_S \sin\phi}\,. \tag{C-11}$$

Note the symmetry in equation (C-11) with respect to the subscripts "P" and "S": the second term can be obtained by interchanging these subscripts in the first term. The expression for D, also needed in equation (C-9), was derived previously [equation (A-19)]:

$$D = 1 + \frac{1}{2}\tan\phi\,(q'_P + q'_S)\,. \tag{C-12}$$

Equations (C-11) and (C-12) are sufficient for obtaining the derivative $dx/dp_{\rm int}$ from equation (C-9).

NMO velocity, as given by equation (C-4), also depends on the minimum traveltime, which can be found from equations (A-4), (A-18), and (A-19):

$$t_{\min} = t(p_{\rm int}^{\min}) = z_{\rm CMP}\ \left.\frac{q_P - p_P q'_P + q_S - p_S q'_S}{1 + \frac{1}{2}\tan\phi\,(q'_P + q'_S)}\right|_{p_{\rm int}^{\min}} . \tag{C-13}$$

Substituting equations (C-8), (C-9) and (C-13) into equation (C-4) and taking into account that at the traveltime minimum $p_P = p_S = p_P^{\min}$ [see equation (C-16) below] yields the final expression for NMO velocity as a function of the horizontal slownesses of the P- and S-waves:

$$V^2_{{\rm nmo},PS} = \left.\frac{4\,(q''_P\,A_S^2 \,+\, q''_S\,A_P^2)}{(A_P + A_S)^2\,[\,p_P\,(q'_P + q'_S) - (q_P + q_S)]}\right|_{p_P^{\min}} , \tag{C-14}$$

where

$$A_P = 1 + q'_P \tan\phi\,, \qquad A_S = 1 + q'_S \tan\phi\,. \tag{C-15}$$

To obtain the ray parameter $p_P^{\min}$, we use equation (C-3) for the slope of the moveout curve. Since at the traveltime minimum the slope goes to zero,

$$p_P^{\min} = p_S^{\min}\,. \tag{C-16}$$

Substituting $p_P = p_S$ into Snell's law [equation (C-5)] and dividing both sides by $\cos\phi$ gives the following equation for the slownesses corresponding to the traveltime minimum:

$$2p_P^{\min} = -(q_P + q_S)\tan\phi\,, \tag{C-17}$$

where the vertical slownesses q_P and q_S are related to $p_P = p_S$ through the Christoffel equation.

For isotropic media, the vertical slownesses are given simply by

$$q_P = \sqrt{\frac{1}{V_P^2} - p_P^2} \tag{C-18}$$

and

$$q_S = \sqrt{\frac{1}{V_S^2} - p_S^2}\ . \tag{C-19}$$

In this case, it is possible to derive an explicit expression for $p_P^{\min} = p_S^{\min}$ by solving equation (C-17) with q_P and q_S from equations (C-18) and (C-19):

$$p_{\text{is}}^{\min} = -\frac{\sin\phi}{2\,V_P}\sqrt{1+\gamma^2+S}\,, \tag{C-20}$$

where $\gamma \equiv V_P/V_S$,

$$S \equiv \sqrt{4\gamma^2 - \tan^2\phi\,(\gamma^2-1)^2}\,, \tag{C-21}$$

and the subscript "is" denotes "isotropic." This solution, however, exists only if the expression under the radical in equation (C-21) is nonnegative, or

$$\tan\phi \le \frac{2\gamma}{\gamma^2-1}\,. \tag{C-22}$$

For larger dip ϕ, the moveout curve has no minimum.

APPENDIX D–WEAK-ANISOTROPY APPROXIMATION FOR MOVEOUT OF CONVERTED WAVES IN VTI MEDIA

Parametric expressions for the traveltime curve

Here we derive weak-anisotropy approximations for traveltime and offset for PS-reflections in VTI media by carrying out linearization in Thomsen's parameters ϵ and δ. For small $|\epsilon| \ll 1$ and $|\delta| \ll 1$, phase velocities of P- and $S(SV)$-waves can be well-approximated by the following linearized expressions (Thomsen 1986):

$$V_P(\hat{\theta}) = V_{P0}\left[1 + \delta \sin^2\hat{\theta} + (\epsilon - \delta)\sin^4\hat{\theta}\right] \tag{D-1}$$

and

$$V_{SV}(\hat{\theta}) = V_{S0}\left(1 + \sigma \sin^2\hat{\theta}\cos^2\hat{\theta}\right), \tag{D-2}$$

where $\hat{\theta}$ is the phase angle with the symmetry axis, and

$$\sigma \equiv \left(\frac{V_{P0}}{V_{S0}}\right)^2(\epsilon - \delta). \tag{D-3}$$

Our first goal is to express the group velocity and group angle for both P- and S-waves (Fig. 3) through the slowness $p_{\rm int}$. Let us denote the angle between the phase-velocity (slowness) vector of the downgoing P-wave and the reflector normal (pointing upward) by $\bar{\theta}_P$ (Fig. D-1). Then the phase angle $\hat{\theta}$ with the symmetry axis is equal to $\bar{\theta}_P - \phi$, and equation (D-1) can be written as

$$V_P(\bar{\theta}_P) = V_{P0}\left[1 + \delta \sin^2(\bar{\theta}_P - \phi) + (\epsilon - \delta)\sin^4(\bar{\theta}_P - \phi)\right]. \tag{D-4}$$

In the linearized weak-anisotropy approximation, group velocity (at the group angle) is equal to phase velocity. Also, we can use the isotropic relationship between the phase angle $\bar{\theta}_P$ and $p_{\rm int}$ because $\bar{\theta}_P$ is contained only in terms already linear in the anisotropic parameters. Hence, the group velocity of the P-wave is given by

$$g_P(p_{\rm int}) = V_{P0}\left[1 + \delta \sin^2(\bar{\theta}_{{\rm is},P} - \phi) + (\epsilon - \delta)\sin^4(\bar{\theta}_{{\rm is},P} - \phi)\right], \tag{D-5}$$

where

$$\sin\bar{\theta}_{\mathrm{is},P} = p_{\mathrm{int}}\, V_{P0}\,; \qquad \cos\bar{\theta}_{\mathrm{is},P} = -\sqrt{1-(p_{\mathrm{int}}\, V_{P0})^2}\,. \tag{D-6}$$

Next, we need to find the P-wave group angle θ_P^{gr} [equation (A-1)] as a function of p_{int}. For the phase angle $\bar{\theta}_P$ we have

$$\sin\bar{\theta}_P = p_{\mathrm{int}}\, V_P = p_{\mathrm{int}}\, V_{P0}\,(1+\alpha_{\mathrm{anis},P}) \tag{D-7}$$

and

$$\cos\bar{\theta}_P = -\sqrt{1-(p_{\mathrm{int}}\, V_{P0})^2}\,\left[1-\frac{(p_{\mathrm{int}}\, V_{P0})^2}{1-(p_{\mathrm{int}}\, V_{P0})^2}\,\alpha_{\mathrm{anis},P}\right], \tag{D-8}$$

where

$$\alpha_{\mathrm{anis},P} \equiv \delta\sin^2(\bar{\theta}_{\mathrm{is},P}-\phi) + (\epsilon-\delta)\sin^4(\bar{\theta}_{\mathrm{is},P}-\phi)\,. \tag{D-9}$$

Using the weak-anisotropy relationship between the group and phase angles in TI media (Thomsen 1986) and taking into account that the P-wave propagates upward from the reflection point yields

$$\tan\theta_P^{\mathrm{gr}} = -\tan(\bar{\theta}_P-\phi)\,[1+2\delta+4(\epsilon-\delta)\sin^2(\bar{\theta}_{\mathrm{is},P}-\phi)]\,. \tag{D-10}$$

Thus, the weak-anisotropy approximation makes it possible to find explicit expressions for group velocity and group angle in terms of the slowness projection p_{int}. Substituting $\sin\bar{\theta}_P$ and $\cos\bar{\theta}_P$ from equations (D-7) and (D-8) into equation (D-10) and further linearizing in the anisotropic parameters, we obtain

$$\begin{aligned}\tan\theta_P^{\mathrm{gr}} = -\tan(\bar{\theta}_{\mathrm{is},P}-\phi)\,\Big[&1+2\delta+4(\epsilon-\delta)\sin^2(\bar{\theta}_{\mathrm{is},P}-\phi)\\ &+\alpha_{\mathrm{anis},P}\,\frac{\tan\bar{\theta}_{\mathrm{is},P}}{\sin(\bar{\theta}_{\mathrm{is},P}-\phi)\cos(\bar{\theta}_{\mathrm{is},P}-\phi)}\Big]\,.\end{aligned} \tag{D-11}$$

From equation (D-10) it also follows that

$$\frac{1}{\cos\theta_P^{\mathrm{gr}}} = -\frac{1}{\cos(\bar{\theta}_P-\phi)}\,\{1+\sin^2(\bar{\theta}_{\mathrm{is},P}-\phi)\,[2\delta+4(\epsilon-\delta)\sin^2(\bar{\theta}_{\mathrm{is},P}-\phi)]\}\,. \tag{D-12}$$

Combining equations (D-5) and (D-12) gives the term $(1/g_P \cos\theta_P^{\rm gr})$ needed to find the traveltime along the P-wave leg:

$$\frac{1}{g_P \cos\theta_P^{\rm gr}} = -\frac{1}{V_{P0}\,\cos(\bar{\theta}_{{\rm is},P} - \phi)} \left[1 + 2(\epsilon - \delta)\sin^4(\bar{\theta}_{\rm is} - \phi) + \alpha_{\rm anis,P}\,\frac{\cos\phi}{\cos\bar{\theta}_{\rm is,P}\,\cos(\bar{\theta}_{{\rm is},P} - \phi)}\right]. \tag{D-13}$$

Similar algebraic transformations yield the corresponding expressions for the S-wave leg:

$$\tan\theta_S^{\rm gr} = \tan(\bar{\theta}_{{\rm is},S} - \phi)\left[1 + 2\sigma - 4\sigma\sin^2(\bar{\theta}_{{\rm is},S} - \phi) + \alpha_{{\rm anis},S}\,\frac{\tan\bar{\theta}_{{\rm is},S}}{\sin(\bar{\theta}_{{\rm is},S} - \phi)\cos(\bar{\theta}_{{\rm is},S} - \phi)}\right], \tag{D-14}$$

$$\frac{1}{g_S \cos\theta_S^{\rm gr}} = \frac{1}{V_{S0}\cos(\bar{\theta}_{{\rm is},S} - \phi)}\left[1 - 2\sigma\sin^4(\bar{\theta}_{{\rm is},S} - \phi) + \alpha_{{\rm anis},S}\,\frac{\cos\phi}{\cos\bar{\theta}_{{\rm is},S}\,\cos(\bar{\theta}_{{\rm is},S} - \phi)}\right], \tag{D-15}$$

where

$$\alpha_{{\rm anis},S} \equiv \sigma\sin^2(\bar{\theta}_{{\rm is},S} - \phi)\cos^2(\bar{\theta}_{{\rm is},S} - \phi) \tag{D-16}$$

and

$$\sin\bar{\theta}_{{\rm is},S} = p_{\rm int}\,V_{S0}\,; \qquad \cos\bar{\theta}_{{\rm is},S} = \sqrt{1 - (p_{\rm int}\,V_{S0})^2}\ . \tag{D-17}$$

Note that the terms involving anisotropic coefficients in equations (D-14) and (D-15) can be found from the anisotropic terms in the corresponding P-wave equations (D-11) and (D-13) by making the following substitutions: V_{P0} should be replaced with V_{S0}, δ – with σ, and ϵ set to zero. Equations (D-11), (D-13), (D-14), and (D-15) are sufficient for obtaining the traveltime and offset for the PS-wave using the general relationships (A-4)–(A-8).

Moveout attributes

Next, with the help of symbolic software Mathematica, we derive the weak-anisotropy approximations for the attributes of the PS traveltime function. The approximate slope of the moveout curve at zero offset can be found by linearizing the exact equation (C-3) in ϵ and δ. From equation (A-17) it follows that for the zero-offset reflection

$$q'_P = q'_S \,, \tag{D-18}$$

because at $x = 0$ the group-velocity vectors of P- and S-waves are parallel to each other. The horizontal slownesses ($p_{_P}$ and $p_{_S}$) also have to satisfy Snell's law [equation (C-5)]. To find $p_{_P}$ and $p_{_S}$, we linearize the vertical slownesses in the anisotropic parameters:

$$q_{_P} = q_{_{P0}} \left\{ 1 - \frac{p_{_P}^2}{q_{_{P0}}^2} \left[\delta + (\epsilon - \delta)\, p_{_P}^2\, V_{P0}^2 \right] \right\} , \tag{D-19}$$

$$q_{_S} = q_{_{S0}} \left(1 - \sigma\, p_{_S}^2\, V_{S0}^2 \right) , \tag{D-20}$$

where

$$q_{_{P0}} = \sqrt{\frac{1}{V_{P0}^2} - p_{_P}^2} \,, \tag{D-21}$$

$$q_{_{S0}} = \sqrt{\frac{1}{V_{S0}^2} - p_{_S}^2} \,. \tag{D-22}$$

Substitution of equations (D-19) and (D-20) into equations (C-5) and (D-18) leads to a system of two equations for the horizontal slownesses $p_{_P}$ and $p_{_S}$. Splitting $p_{_P}$ and $p_{_S}$ into the isotropic and anisotropic parts, solving this system, and using the obtained horizontal slownesses in equation (C-3) yields

$$\begin{aligned} \left.\frac{dt}{dx}\right|_{x=0} &= \frac{\sin\phi}{2\, V_{P0}\,(1+\gamma)} \left[(1-\gamma^2) + 4\gamma\,(\sigma - \delta) \right] \\ &+ \frac{\sin^3\phi}{2\, V_{P0}\,\gamma\,(1+\gamma)} \left[\delta\gamma\,(1+\gamma) - \sigma\,(\gamma^3 + 9\gamma^2 + 8) \right] \\ &+ \frac{\sin^5\phi}{2\, V_{P0}\,\gamma^2\,(1+\gamma)}\, \sigma\,(\gamma^4 + 5\gamma^3 + 5\gamma + 1) \,; \end{aligned} \tag{D-23}$$

$\gamma \equiv V_{P0}/V_{S0}$.

To find the attributes of the traveltime minimum, we need to determine the corresponding horizontal slowness $p_P^{\min} = p_S^{\min}$. The linearized form of $p_P^{\min}$ can be found from Snell's law [equation (C-17)] by substituting the approximations for the vertical slownesses [equations (D-19) and (D-20)]:

$$p_P^{\min} = p_{\rm is}^{\min}\,(1 + \Delta p_P^{\min})\,, \tag{D-24}$$

where $p_{\rm is}^{\min}$ is the isotropic solution [equation (C-20)] and

$$\Delta p_P^{\min} = -\frac{\tan\phi}{2p_{\rm is}^{\min}}\,\left(q_{P0}\,\Delta q_P + q_{S0}\,\Delta q_S\right)\,. \tag{D-25}$$

Here q_{P0} and q_{S0} are given by equations (D-21) and (D-22) with $p_P = p_S = p_{\rm is}^{\min}$, and

$$\Delta q_P = \frac{(p_{\rm is}^{\min})^2}{q_{P0}^2}\,[\delta + (\epsilon - \delta)\,(p_{\rm is}^{\min})^2\,V_{P0}^2]\,, \tag{D-26}$$

$$\Delta q_S = \sigma\,(p_{\rm is}^{\min})^2\,V_{S0}^2\,. \tag{D-27}$$

If necessary, the slowness projection on the interface corresponding to the traveltime minimum can be found from equation (D-24) as

$$p_{\rm int}^{\min} = \frac{\sin\phi}{2}\,\left(\frac{1}{V_{S0}} - \frac{1}{V_{P0}}\right)\,, \tag{D-28}$$

where only the leading dip term was retained. Equation (D-28) is fully equivalent to the isotropic result (C-20).

To obtain the weak-anisotropy approximation for normal-moveout velocity, we linearize the exact equation (C-14) in the anisotropic parameters. Expanding the linearized version of equation (C-14) in $\sin\phi$ up to the quadratic term and substituting $p_P^{\min}$ from equation (D-24) leads to the following form of $V_{{\rm nmo},PS}$:

$$\begin{aligned} V_{{\rm nmo},PS}^{-2} = {} & \frac{1}{V_{P0}V_{S0}} - \frac{\sin^2\phi}{8\,V_{P0}^3V_{S0}^3}\,\left[3\,V_{P0}^4 - 2\,V_{P0}^3V_{S0} + 6\,V_{P0}^2V_{S0}^2 - 2\,V_{P0}V_{S0}^3 + 3\,V_{S0}^4\right] \\ & + \frac{\epsilon}{2\,V_{P0}V_{S0}^4(V_{P0}+V_{S0})}\,\Big[-4\,V_{P0}^2V_{S0}^2 + \sin^2\phi\,(3\,V_{P0}^4 - 11\,V_{P0}^3V_{S0} \end{aligned}$$

$$-V_{P0}^2V_{S0}^2+3\,V_{P0}V_{S0}^3+6\,V_{S0}^4)\Big]$$
$$+\frac{\delta\,(V_{S0}-V_{P0})}{2\,V_{P0}^2V_{S0}^4(V_{P0}+V_{S0})}\Big[-4\,V_{P0}^2V_{S0}^2+\sin^2\phi\,(3\,V_{P0}^4-8\,V_{P0}^3V_{S0}$$
$$-6\,V_{P0}^2V_{S0}^2-8\,V_{P0}V_{S0}^3+3\,V_{S0}^4)\Big]\,. \tag{D-29}$$

It is convenient to describe the moveout attributes in terms of the ray parameter (horizontal slowness) of the pure P-wave reflection recorded at zero offset ($p_{_{P0}}$). Neglecting the cubic and higher powers of $\sin\phi$, we can represent $p_{_{P0}}$ as

$$p_{_{P0}}=\frac{\sin\phi}{V_P(\phi)}\approx\frac{\sin\phi}{V_{P0}}\,. \tag{D-30}$$

Equation (D-30) has a purely "isotropic" form because the anisotropic terms in $p_{_{P0}}$ are multiplied with high powers of $\sin\phi$ not included in our approximation.

Substituting γ and $p_{_{P0}}$ and expressing ϵ through σ yields the following expression for NMO velocity:

$$V_{\rm nmo,PS}^{-2}\,(p_{_{P0}})=V_{\rm nmo,PS}^{-2}(0)-\frac{p_{_{P0}}^2}{8\gamma}\,(3\gamma^4-2\gamma^3+6\gamma^2-2\gamma+3)$$
$$-\;\frac{p_{_{P0}}^2\,(\gamma-1)}{2\gamma\,(\gamma+1)}\Big[6\,\sigma\,(\gamma+1)^2-(\sigma-\delta)\,\gamma\,(3\gamma^2-2\gamma+3)\Big]\,, \tag{D-31}$$

where

$$V_{\rm nmo,PS}^{-2}(0)=\frac{1}{V_{P0}V_{S0}}\,\left[1-\frac{2(\sigma+\delta\gamma)}{1+\gamma}\right]\,. \tag{D-32}$$

The approximate normalized offset $x_{\rm min}/t_{\rm min}$ is obtained in a similar way. Linearizing the exact equation (20) for $x_{\rm min}/t_{\rm min}$, substituting $p_P^{\rm min}$ [equation (D-24)] and retaining only the linear and cubic terms in $\sin\phi$, we find

$$\frac{x_{\rm min}}{t_{\rm min}}=\frac{\sin\phi\;V_{S0}}{2}\Big[\gamma-1+2(\delta\gamma-\sigma)\Big]+\frac{\sin^3\phi\;V_{S0}}{16\,\gamma^2}\Big[(\gamma^5+3\gamma^3-3\gamma^2-1)$$
$$+\,4\delta\gamma^3(\gamma^2+1)+4\sigma(2\gamma^3+5\gamma^2+6\gamma+1)\Big]\,. \tag{D-33}$$

Likewise, the leading dip term in the weak-anisotropy approximation for the spatial derivative of the minimum traveltime (21) is given by

$$\frac{dt_{\rm min}}{dy_{\rm CMP}}=\tan\phi\,\frac{dt_{\rm min}}{dz_{\rm CMP}}=p_{_{P0}}\,(1+\gamma)\,. \tag{D-34}$$

REFERENCES

Alfaraj M.N. 1993. *Transformation to zero offset for mode-converted waves.* Ph.D. thesis, Colorado School of Mines.

Alkhalifah T., Tsvankin I., Larner K. and Toldi J. 1996. Velocity analysis and imaging in transversely isotropic media: Methodology and a case study. *The Leading Edge* **15**, no. 5, 371–378.

Alkhalifah T. and Tsvankin I. 1995. Velocity analysis for transversely isotropic media. *Geophysics* **60**, 1550–1566.

Anderson J.E. 1996. *Imaging in transversely isotropic media with a vertical symmetry axis.* Ph.D. thesis, Colorado School of Mines.

Cohen J.K. 1998. A convenient expression for the NMO velocity function in terms of ray parameter. *Geophysics* **63**, 275–278.

Grechka V., Theophanis S. and Tsvankin I. 1999. Joint inversion of P- and PS-waves in orthorhombic media: Theory and a physical-modeling study. *Geophysics* **64**, 146–161.

Grechka V. and Tsvankin I. 1998. 3-D description of normal moveout in anisotropic inhomogeneous media. *Geophysics* **63**, 1079–1092.

Grechka V. and Tsvankin I. 1999. Inversion of azimuthally dependent NMO velocity in transversely isotropic media with a tilted axis of symmetry: *Geophysics*, in print.

Grechka V., Tsvankin I. and Cohen, J.K. 1999. Generalized Dix equation and analytic treatment of normal-moveout velocity for anisotropic media. *Geophysical Prospecting* **47**, 117–148.

Hubral P. and Krey T. 1980. *Interval velocities from seismic reflection measurements*. Soc. Expl. Geophys.

Rommel B. 1997. Stacking charts for converted waves in a transversely isotropic medium. CWP Research Report (CWP-252).

Seriff A.J. and Sriram K.P. 1991. *P-SV* reflection moveouts for transversely isotropic media with a vertical symmetry axis. *Geophysics* **56**, 1271–1274.

Tessmer G. and Behle A. 1988. Common reflection point data-stacking technique for converted waves. *Geophysical Prospecting*, **36**, 671–688.

Thomsen L. 1986. Weak elastic anisotropy. *Geophysics* **51**, 1954–1966.

Tsvankin I. 1995. Normal moveout from dipping reflectors in anisotropic media. *Geophysics* **60**, 268–284.

Tsvankin I. 1996. *P*-wave signatures and notation for transversely isotropic media: An overview. *Geophysics* **61**, 467–483.

Tsvankin I. 1997. Anisotropic parameters and *P*-wave velocity for orthorhombic media. *Geophysics* **62**, 1292–1309.

Tsvankin I. and Thomsen L. 1994. Nonhyperbolic reflection moveout in anisotropic media. *Geophysics* **59**, 1290–1304.

Tsvankin I. and Thomsen L. 1995. Inversion of reflection traveltimes for transverse isotropy. *Geophysics* **60**, 1095–1107.

FIGURES

FIG. 1. Dip-line reflection moveout of a PS-wave in a homogeneous VTI layer with the parameters $V_{P0} = 2.0$ km/s, $V_{S0} = 1.0$ km/s, $\epsilon = 0.2$, $\delta = 0.1$ ($\sigma = 0.4$); the distance between the CMP and the reflector is 1 km. Reflector dip is shown on top of each plot. Positive offsets correspond to the P-wave source located downdip from the CMP.

FIG. 2. Dip-line moveout of a PS-wave in a VTI layer with the parameters $V_{P0} = 2.0$ km/s, $V_{S0} = 1.2$ km/s, $\epsilon = 0.3$, $\delta = 0.05$ ($\sigma = 0.69$); the distance between the CMP and the reflector is 1 km.

FIG. 3. Reflected PS-wave in a symmetry plane of an anisotropic medium. $\vec{g}_P$ and $\vec{g}_S$ are the group-velocity vectors (rays) of the P- and S-waves, $\theta_P^{\rm gr}$ and $\theta_S^{\rm gr}$ are the corresponding group angles with vertical, $z_{\rm CMP}$ is the reflector depth beneath the CMP, and z_r is the depth of the reflection point. In the parametric moveout equations it is assumed that $\vec{g}_P$ and $\vec{g}_S$ point towards the surface. The horizontal ray displacements are $x_P = SN$ and $x_S = NR$.

FIG. 4. Exact slope of the PS-wave moveout curve at zero offset [equation (10), solid line] and its weak-anisotropy approximation [equation (22), dotted line] in two VTI models: (a) $\epsilon = 0.15$, $\delta = 0.05$ ($\sigma = 0.28$); (b) $\epsilon = 0.3$, $\delta = 0.05$ ($\sigma = 0.69$). For both media, $V_{P0} = 2.0$ km/s and $V_{S0} = 1.2$ km/s. Reflector dip changes from 0° to 50° in accordance with the product $p_{_{P0}} V_{P0}$, approximated here by $\sin\phi$. Moveout curves for Model b are shown in Fig. 2.

FIG. 5. Exact NMO velocity of the PS-wave [equation (15), solid line] and its weak-anisotropy approximation [equation (26), dotted line] in two VTI models: (a) $\epsilon = \delta = 0.15$ (elliptical anisotropy); (b) $\epsilon = 0.15$, $\delta = 0.05$. For both media, $V_{P0} = 2.0$

km/s and $V_{S0} = 1.2$ km/s. Reflector dip changes from 0° to 30°.

FIG. 6. Exact reflection moveout of the PS-wave (solid) and its approximation with the best-fit shifted hyperbola (31) (dashed) found by least-squares minimization. The model parameters are $V_{P0} = 2.0$ km/s, $V_{S0} = 1$ km/s, $\epsilon = 0.2$, $\delta = 0.1$, $\phi = 30°$.

FIG. 7. Ray-traced synthetic seismograms of the PS-wave reflected from the bottom of a VTI layer. The dip ϕ of the reflector is shown on top of each plot. The parameters of the upper layer are $V_{P0} = 2.0$ km/s, $V_{S0} = 1$ km/s, $\epsilon = 0.2$, $\delta = 0.1$, the density $\rho = 2$ g/cm^3. The lower layer is isotropic with $V_{P0} = 2.2$ km/s, $V_{S0} = 1.1$ km/s and $\rho = 2.2$ g/cm^3. Only positive offsets (with the P-wave source located downdip from the CMP) are displayed.

FIG. 8. Parameters ϵ, δ, V_{P0}, and V_{S0} (dots) determined by inverting P and PS moveout data from a horizontal and dipping reflector. The input data were distorted by random noise with a standard deviation of 0.5% for γ, 1.5% for the zero-dip NMO velocities and 2% for the moveout attributes of the dipping event. (a) and (b) Inversion *without* dip-moveout attributes of the PS-wave; the dip $\phi = 30°$. (c) and (d) Inversion including the dip-moveout attributes of the traveltime minimum of the PS-wave and the slope of the PS-moveout curve [equation (35)]; the dip $\phi = 30°$. (e) and (f) Inversion including the slope of the PS-moveout curve [equation (36)]; the dip $\phi = 50°$. The actual values are: $V_{P0} = 2.0$ km/s, $V_{S0} = 1$ km/s, $\epsilon = 0.2$, $\delta = 0.1$. The solid line on plot (a) indicates ϵ's and δ's corresponding to the correct value of η ($\eta = 0.083$).

FIG. B-1. To determine the slope of the moveout curve at the offset $x_0 = SR$, the specular reflection raypath $S_1O_1R_1$ in a vicinity of x_0 can be replaced by a non-specular raypath S_1OR_1.

FIG. D-1. Geometry for the derivation of the weak-anisotropy approximation for PS moveout. OP and OS are the slowness (phase-velocity) directions of the downgoing P- and upgoing S-legs of the converted wave, and $\bar{\theta}_P$ and $\bar{\theta}_S$ are the corresponding phase (slowness) angles with the reflector normal ON. OM, the projection of the slowness vectors on the reflector (denoted as p_{int}), should be identical for the P- and S-waves.

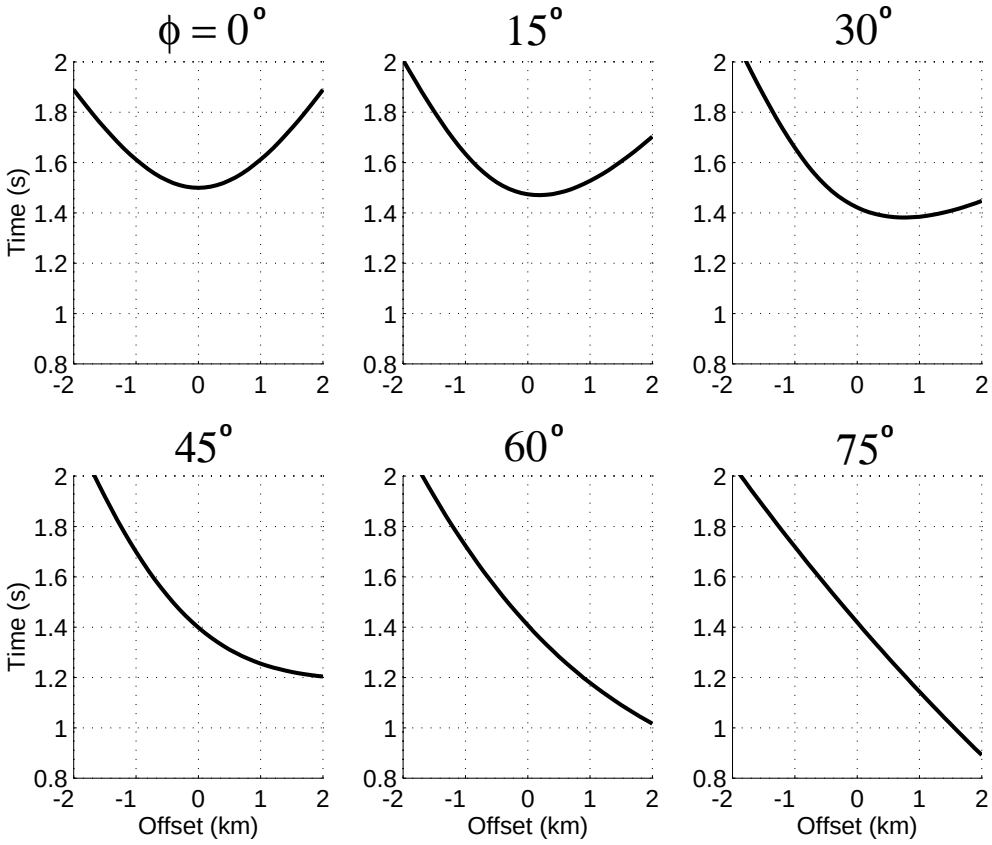

FIG. 1. Dip-line reflection moveout of a PS-wave in a homogeneous VTI layer with the parameters $V_{P0} = 2.0$ km/s, $V_{S0} = 1.0$ km/s, $\epsilon = 0.2$, $\delta = 0.1$ ($\sigma = 0.4$); the distance between the CMP and the reflector is 1 km. Reflector dip is shown on top of each plot. Positive offsets correspond to the P-wave source located downdip from the CMP.

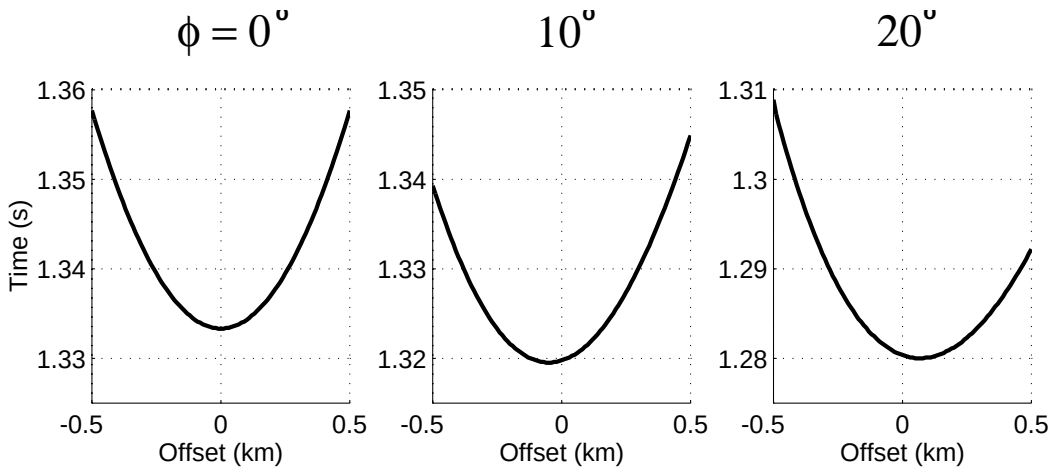

FIG. 2. Dip-line moveout of a PS-wave in a VTI layer with the parameters $V_{P0} = 2.0$ km/s, $V_{S0} = 1.2$ km/s, $\epsilon = 0.3$, $\delta = 0.05$ ($\sigma = 0.69$); the distance between the CMP and the reflector is 1 km.

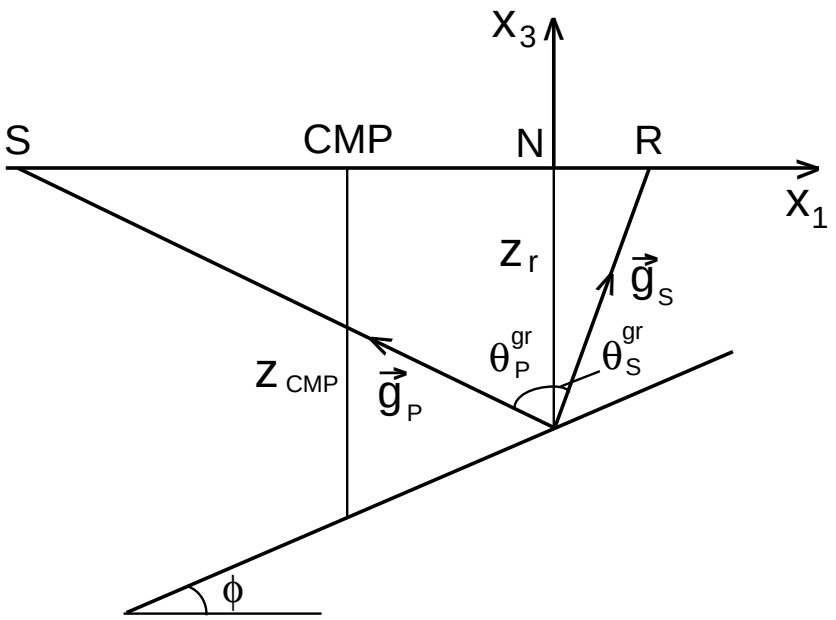

FIG. 3. Reflected PS-wave in a symmetry plane of an anisotropic medium. $\vec{g}_P$ and $\vec{g}_S$ are the group-velocity vectors (rays) of the P- and S-waves, $\theta_P^{\rm gr}$ and $\theta_S^{\rm gr}$ are the corresponding group angles with vertical, $z_{\rm CMP}$ is the reflector depth beneath the CMP, and z_r is the depth of the reflection point. In the parametric moveout equations it is assumed that $\vec{g}_P$ and $\vec{g}_S$ point towards the surface. The horizontal ray displacements are $x_P = SN$ and $x_S = NR$.

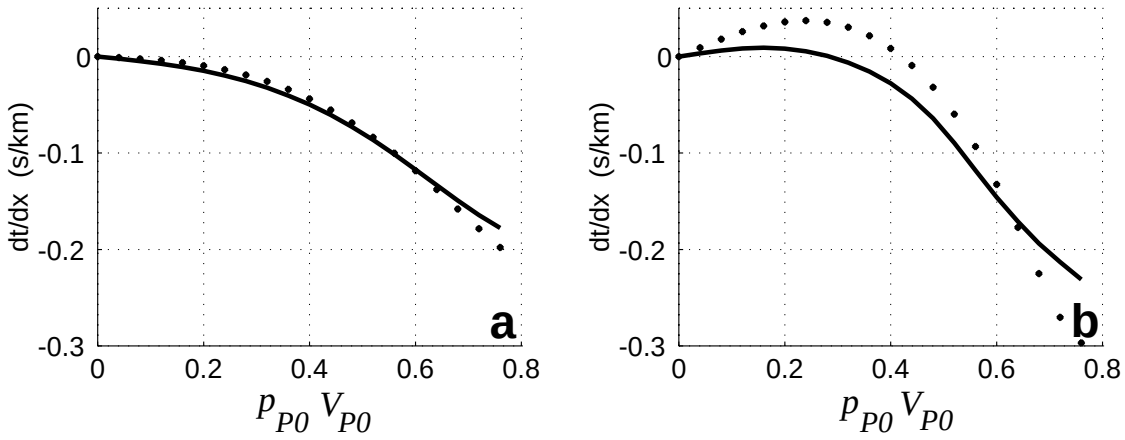

FIG. 4. Exact slope of the PS-wave moveout curve at zero offset [equation (10), solid line] and its weak-anisotropy approximation [equation (22), dotted line] in two VTI models: (a) $\epsilon = 0.15$, $\delta = 0.05$ ($\sigma = 0.28$); (b) $\epsilon = 0.3$, $\delta = 0.05$ ($\sigma = 0.69$). For both media, $V_{P0} = 2.0$ km/s and $V_{S0} = 1.2$ km/s. Reflector dip changes from 0° to 50° in accordance with the product $p_{P0}\,V_{P0}$, approximated here by $\sin\phi$. Moveout curves for Model b are shown in Fig. 2.

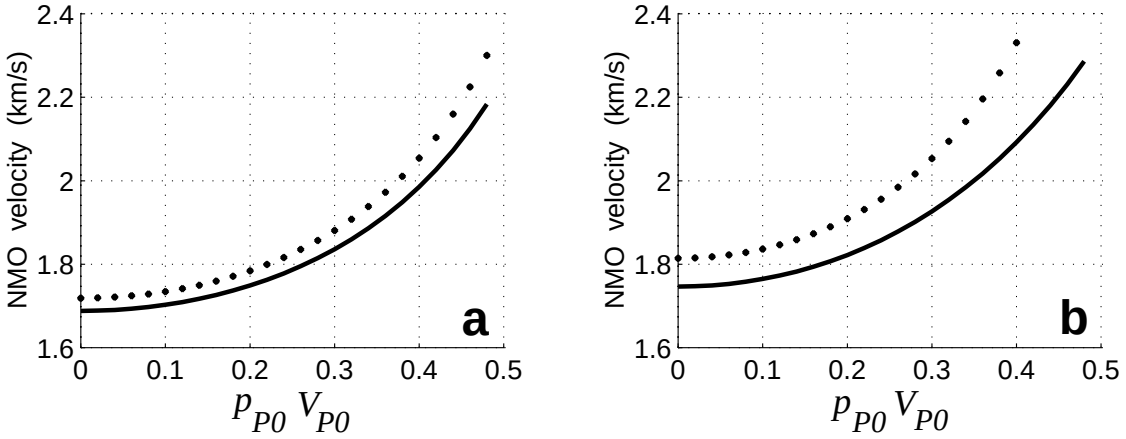

FIG. 5. Exact NMO velocity of the PS-wave [equation (15), solid line] and its weak-anisotropy approximation [equation (26), dotted line] in two VTI models: (a) $\epsilon = \delta = 0.15$ (elliptical anisotropy); (b) $\epsilon = 0.15$, $\delta = 0.05$. For both media, $V_{P0} = 2.0$ km/s and $V_{S0} = 1.2$ km/s. Reflector dip changes from 0° to 30°.

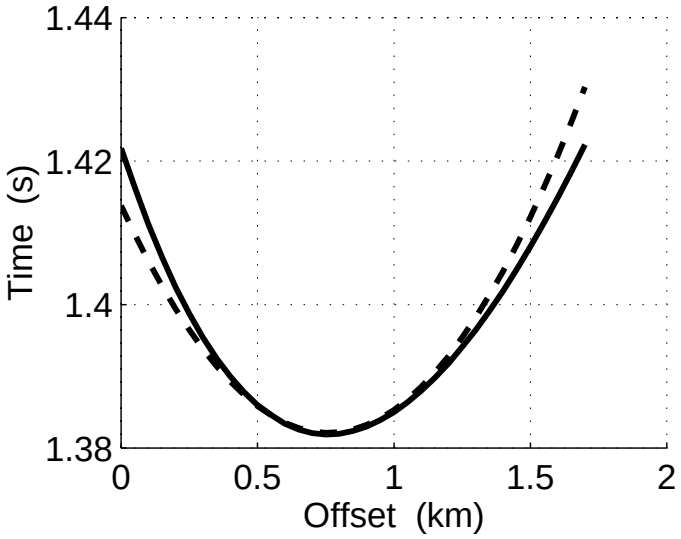

FIG. 6. Exact reflection moveout of the PS-wave (solid) and its approximation with the best-fit shifted hyperbola (31) (dashed) found by least-squares minimization. The model parameters are $V_{P0} = 2.0$ km/s, $V_{S0} = 1$ km/s, $\epsilon = 0.2$, $\delta = 0.1$, $\phi = 30^\circ$.

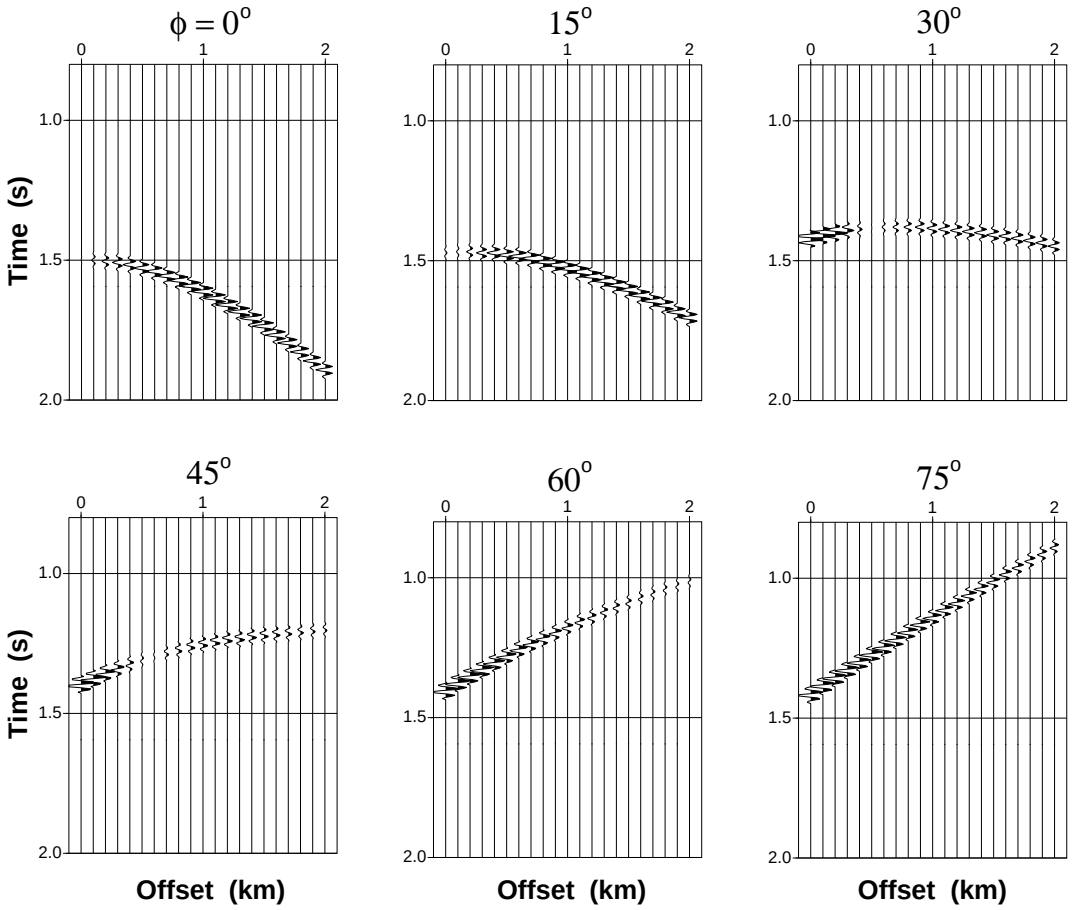

FIG. 7. Ray-traced synthetic seismograms of the PS-wave reflected from the bottom of a VTI layer. The dip ϕ of the reflector is shown on top of each plot. The parameters of the upper layer are $V_{P0} = 2.0$ km/s, $V_{S0} = 1$ km/s, $\epsilon = 0.2$, $\delta = 0.1$, the density $\rho = 2$ g/cm^3. The lower layer is isotropic with $V_{P0} = 2.2$ km/s, $V_{S0} = 1.1$ km/s and $\rho = 2.2$ g/cm^3. Only positive offsets (with the P-wave source located downdip from the CMP) are displayed.

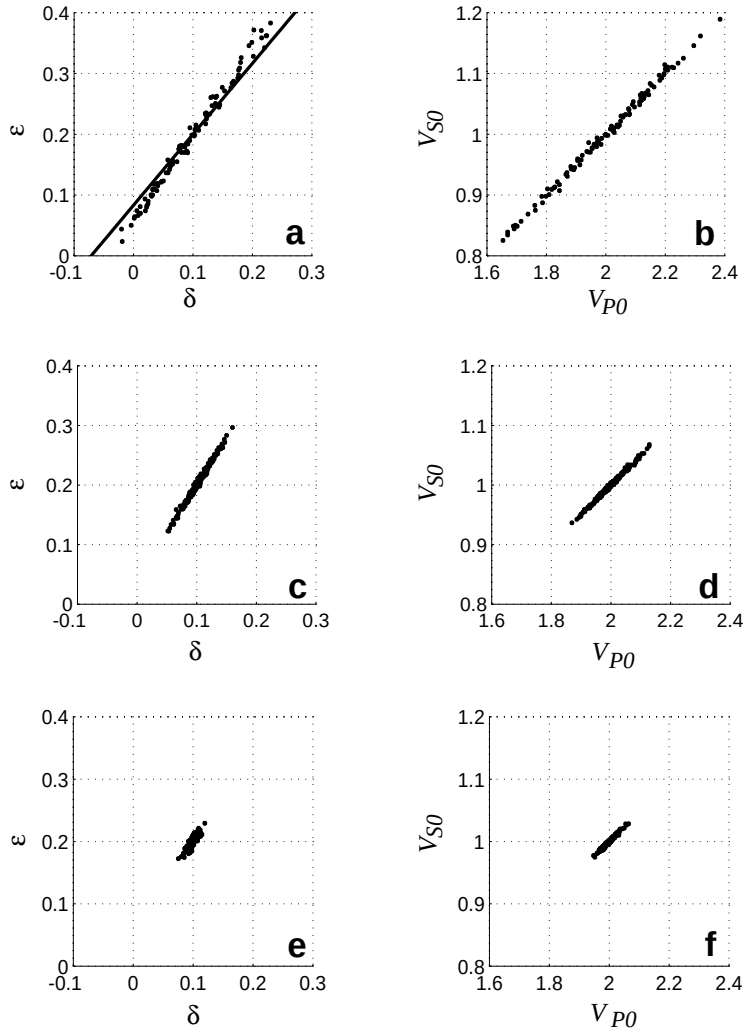

FIG. 8. Parameters ϵ, δ, V_{P0}, and V_{S0} (dots) determined by inverting P and PS moveout data from a horizontal and dipping reflector. The input data were distorted by random noise with a standard deviation of 0.5% for γ, 1.5% for the zero-dip NMO velocities and 2% for the moveout attributes of the dipping event. (a) and (b) Inversion *without* dip-moveout attributes of the PS-wave; the dip $\phi = 30°$. (c) and (d) Inversion including the dip-moveout attributes of the traveltime minimum of the PS-wave and the slope of the PS-moveout curve [equation (35)]; the dip $\phi = 30°$. (e) and (f) Inversion including the slope of the PS-moveout curve [equation (36)]; the dip $\phi = 50°$. The actual values are: $V_{P0} = 2.0$ km/s, $V_{S0} = 1$ km/s, $\epsilon = 0.2$, $\delta = 0.1$. The solid line on plot (a) indicates ϵ's and δ's corresponding to the correct value of η ($\eta = 0.083$).

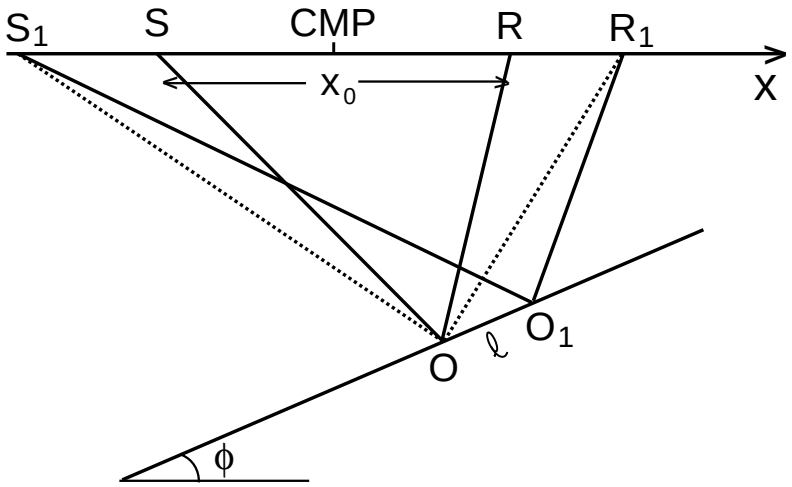

FIG. B-1. To determine the slope of the moveout curve at the offset $x_0 = SR$, the specular reflection raypath $S_1O_1R_1$ in a vicinity of x_0 can be replaced by a non-specular raypath S_1OR_1.

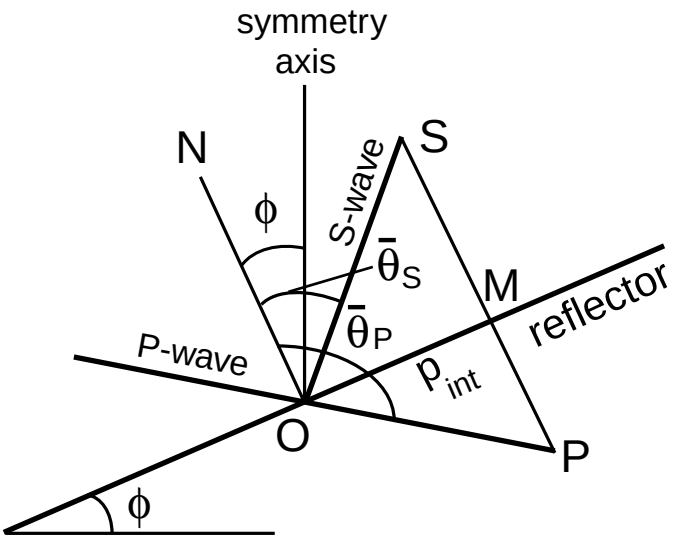

FIG. D-1. Geometry for the derivation of the weak-anisotropy approximation for PS moveout. OP and OS are the slowness (phase-velocity) directions of the downgoing P- and upgoing S-legs of the converted wave, and $\bar{\theta}_P$ and $\bar{\theta}_S$ are the corresponding phase (slowness) angles with the reflector normal ON. OM, the projection of the slowness vectors on the reflector (denoted as $p_{\rm int}$), should be identical for the P- and S-waves.